

Research Article

Predicting the global distribution and invasion scenarios of the Spotted Lanternfly, *Lycorma delicatula* (White, 1845) (Hemiptera, Fulgoridae)

Enrico Ruzzier^{1,2}, Davide Scaccini³, Pietro Tirozzi⁴, Valerio Orioli⁴, Olivia Dondina^{2,4}, Andrea Di Giulio^{1,2}, Alberto Pozzebon³, Luciano Bani^{2,3}

¹ Department of Science, Roma Tre University, Rome, Italy

² National Biodiversity Future Center (NBFC), Palermo, Italy

³ Department of Agronomy, Food, Natural resources, Animals, Environment (DAFNAE), University of Padua, Padova, Italy

⁴ Department of Earth and Environmental Sciences, University of Milano-Bicocca, Milan, Italy

Corresponding authors: Enrico Ruzzier (enrico.ruzzier@uniroma3.it); Olivia Dondina (olivia.dondina@unimib.it)

Abstract

Lycorma delicatula is a species native to the PR of China that has become invasive in South Korea, Japan, and the United States. It is considered a significant threat to agriculture, particularly the viticulture industry, and its further spread into new areas could exacerbate its economic impact. Species Distribution Models (SDMs) are commonly used to analyze the distribution of invasive species, and while *L. delicatula* has already been studied using this spatial modeling approach, previous research has mostly focused on the effects of bioclimatic variables, often overlooking the role of habitat characteristics, including the presence of host plants. In our study, to assess the presence of other suitable habitats for the species on a global scale, we developed a two-step SDM calibrated within its native range, within biogeographic barriers. In the first step, we built two separate models: one for habitat suitability (HSM), incorporating land cover, elevation, and host plants, and another for bioclimatic suitability (BSM). The HSM calibration included the allocation of a portion of pseudo-absences (PAs) along background points (BPs) to mitigate the sampling bias of occurrences concentrated in highly urbanized areas (one bias-controlled PA for every four random BPs). In contrast, the BSM calibration was performed using a fully random allocation of BPs. In the second step, the two models were combined to produce an overall suitability map for the native range, which demonstrated excellent validation performance. When projected globally, the model confirmed that the species has already colonized suitable areas. Beyond the currently invaded regions (i.e., North America and East Asia), the model identifies additional colonizable areas exclusively in Europe. To evaluate the invasion dynamics in both currently invaded regions and potential future invasion areas in Europe, we developed a resistance-distance constrained dispersal model based on a) environmental resistance, derived from the overall suitability map produced by the SDM, and b) intrinsic dispersal distance, estimated from the temporal progression of occurrences in the primary invasion area in the eastern United States. The maximum annual dispersal distance was estimated to be approximately 25 kilometers. Given its relatively low annual dispersal capacity, the species appears capable of naturally spreading within areas of medium to high suitability, while its potential for expansion into low-suitability areas remains quite limited. Medium- and high-suitability regions where the species is already present are likely to undergo significant colonization over the next 10 years. In contrast, adventive populations in low-suitability areas seem unable to expand successfully without human-mediated translocations. In the absence of an adaptive capacity to thrive in ecological contexts different from its native range (niche change or niche shift), the species appears to be a relatively modest invader beyond its currently invaded



Academic editor: Samuel Ward

Received: 29 March 2025

Accepted: 11 September 2025

Published: 4 November 2025

Citation: Ruzzier E, Scaccini D, Tirozzi P, Orioli V, Dondina O, Di Giulio A, Pozzebon A, Bani L (2025) Predicting the global distribution and invasion scenarios of the Spotted Lanternfly, *Lycorma delicatula* (White, 1845) (Hemiptera, Fulgoridae). NeoBiota 103: 267–298. <https://doi.org/10.3897/neobiota.103.154246>

Copyright: © Enrico Ruzzier et al.

This is an open access article distributed under terms of the Creative Commons Attribution License (Attribution 4.0 International – CC BY 4.0).

areas or Europe. Successfully managing the invasion of *L. delicatula* therefore depends on the implementation of early detection and eradication measures, which should be deployed as promptly as possible, especially in highly suitable introduction areas.

Key words: Auchenorrhyncha, bioclimatic suitability model, habitat suitability model, host plants, insect pest, invasive species, Resistance-Distance Constrained Dispersal Model, Species Distribution Model (SDM)

Introduction

The Spotted Lanternfly, *Lycorma delicatula* (White, 1845) (Hemiptera: Fulgoridae) is a planthopper endemic to the PR of China that has become widely invasive in Japan, South Korea, and the United States (Lee et al. 2019; Urban and Leach 2023). The species is of primary phytosanitary concern given its impact on crop production caused by feeding nymphs and adults (Lee et al. 2019; Urban and Leach 2023; Zhang et al. 2023). Indeed, both nymphs and adults of *L. delicatula* feed on plant sap, affecting the health of the plant (Dara et al. 2015). Furthermore, the gregarious behavior of this species, with aggregations of hundreds of individuals, further amplifies the damage to the host plant (Lee et al. 2019). *Lycorma delicatula* is widely polyphagous, feeding on multiple plant species, both in its native and invaded range (CABI 2020; Jung et al. 2022; EPPO 2023), although *Ailanthus altissima* (Mill.) Swingle (commonly known as Tree of Heaven) is often referred to as the primary or preferred host (Nixon et al. 2022; Elsensohn et al. 2023). As a consequence, this insect currently occurs in various anthropogenic environments, such as agricultural and urban areas, as well as in natural and semi-natural habitats (Urban and Leach 2023).

Although the Spotted Lanternfly is potentially harmful to many plant species, multiple studies carried out in the invaded areas have shown that *L. delicatula* is only moderately harmful to hardwood and fruit trees (Hoover et al. 2023; Nixon et al. 2023a) while it is a primary pest on grapevine plants (*Vitis* spp.) (Harner et al. 2022). In the eastern United States, *L. delicatula* prefers vineyard-dominated landscapes (Harner et al. 2022) where it significantly contributes to yield losses and grapevine decline (Urban 2020). These conditions, therefore, make this pest a real threat to the wine and grape industry on a global scale, both in countries where it has already been introduced and in those where it could be in the near future (e.g., Reynolds et al. 2021; Jones et al. 2022; EPPO 2023). Management of this pest predominantly relies on increased use of broad-spectrum insecticides with high residual toxicity, posing significant threats to beneficial non-target organisms and the environment (Lee et al. 2019; Urban and Leach 2023). However, this type of management may be ineffective over the long term, as treated areas can be recolonized by resident populations in adjacent non-crop habitats (Park et al. 2009).

It is crucial to determine the potential distribution of *L. delicatula* on a global scale to identify the areas with the highest establishment risk and to guide more effective early detection strategies and pest management actions (Urban and Leach 2023). In this regard, species distribution models (SDMs) have become effective tools for forecasting the potential distribution of invasive insects (e.g., Elith 2017). To date, several studies predicted the distribution of *L. delicatula* through SDMs, both locally and globally, albeit through different approaches and datasets (Jung et

al. 2017; Namgung et al. 2020; Wakie et al. 2020; Huron et al. 2022; Chartois et al. 2024; Zhao et al. 2024). In addition, Jones et al. (2022) and Montgomery et al. (2023), beyond assessing species suitability, also estimated the risk of invasion by accounting for connectivity under current and future scenarios. These studies, in some cases, estimated suitability based on bioclimatic variables, while in others, they employed a modelling framework that tended to overemphasize the influence of these variables over habitat features (e.g., elevation, host plants). As a result, the interpretation of *L. delicatula* potential distribution is often confined to a broad scenopoetic context rather than a local scale. Recent studies highlight that incorporating habitat variables into a two-step framework, separating a habitat suitability model (HSM) from a bioclimatic suitability model (BSM), enhances SDM forecasting (Adde et al. 2023; Ruzzier et al. 2024). For phytophagous species, integrating host plants into habitat modelling improves the reliability of predictions for potentially suitable areas, both within and outside the native range of the target species (Dang et al. 2021; Ruzzier et al. 2024, 2025).

Studies analyzing the movements of adult females in search of oviposition sites (Wolfen et al. 2019) or food resources (Wolfen et al. 2020) highlight the low propensity of *L. delicatula* to cover long distances. However, the dispersal potential of propagules remains unknown. Gaining insight into the spatial expansion dynamics of propagules could support the development of effective containment strategies, particularly in relation to already infested areas and the suitability of adjacent habitats.

The aims of this research were:

- 1) to separately calibrate a BSM and a HSM within the native range of *L. delicatula* as a basis to produce an overall environmental suitability map;
- 2) to forecast suitable areas for the species at global scale based on the models (BSM and HSM) calibrated to the native range, with a particular focus on invaded and newly colonized areas;
- 3) to evaluate the model effectiveness in predicting the current distribution of this species in invaded areas (USA and South Korea);
- 4) to estimate the annual dispersal distance of *L. delicatula* based on repository occurrences;
- 5) to model the invasion range expansion and forecast the future USA, South Korea and Japan invasion scenarios, as well as the potential invasion scenario in Europe.

Materials and methods

Species occurrences

Occurrences of *L. delicatula* in its native and invaded ranges were retrieved from the Global Biodiversity Information Facility (GBIF) (<https://doi.org/10.15468/dl.azzdjh>; 32,752 occurrences) and iNaturalist (41,867 occurrences), accounting for 74,619 occurrences worldwide. The occurrence data used in the SDMs were updated to October 11, 2024. The dataset was checked for all potential issues (e.g., duplicate records, misidentifications, etc.). For the BSM calibration on native range (mainland PR of China), we used all available occurrences, while for the HSM, we used a subset of the previous data, selecting only those with coordinates in degrees with at least two decimal places of resolution or accuracy lower than

2.5 km (half of the raster cell size of the environmental layers used in the HSM model) (Ruzzier et al. 2025). The rationale of the procedure relies on the capability of associating each occurrence with habitat data derived from land cover cartography with a grid resolution of 0.04167° (corresponding to approximately 5 km at the equator). For BSM, occurrences with higher uncertainty were also included, as bioclimatic variables tend to exhibit greater spatial inertia in their variability. The overall dataset was thinned through the function “ensemble.spatialThin” of the package “*BiodiversityR*” (Kindt and Coe 2005), with a thinning parameter of 2.5 km in R, version 4.4.2 (R Core Team 2023) to exclude duplicated data and remove occurrences within the same raster cell. For HSM and BSM 324 and 402 occurrences were used, respectively.

Occurrences from Japan, the Korean peninsula, and Taiwan were excluded from the analyses since these areas are outside the putative native range of this species; in these countries, *L. delicatula* is naturally absent, because of the existence of major biogeographic barriers (ocean and mountain ranges) that the species is unable to overcome, whereas present occurrences are the result of human introduction.

Bioclimatic, elevation and habitat variables

Bioclimatic (19 strata) and elevation (i.e., digital elevation model, DEM) layers were downloaded from WorldClim 2.1 (available at: <http://www.worldclim.com/version2>) and averaged for the years 1970–2000, with a grid resolution of 0.00833° . Since most Bioclimatic strata are strongly collinear, a preselection of bioclimatic variables may help in reducing multicollinearity, improving model interpretability, and enhancing predictive accuracy (Dormann et al. 2013; Plischoff et al. 2014). We preselected a subset of 10 among them: mean diurnal range (mean of monthly (max temperature – min temperature)) [BIO2]; max temperature of warmest month [BIO5]; min temperature of coldest month [BIO6]; mean temperature of warmest quarter [BIO10]; mean temperature of coldest quarter [BIO11]; annual precipitation [BIO12]; precipitation of wettest quarter [BIO16]; precipitation of driest quarter [BIO17]; precipitation of warmest quarter [BIO18]; precipitation of coldest quarter [BIO19].

Habitat variables were retrieved from The Global 1-km Consensus Land Cover available at <http://www.earthenv.org>. Data were represented by 12 layers (evergreen/deciduous needleleaf trees [EDNT], evergreen broadleaf trees [EBT], deciduous broadleaf trees [DBT], mixed/other trees [MOT], shrubs [SHR], herbaceous vegetation [HERB], cultivated and managed vegetation [CMV], regularly flooded vegetation [RFV], urban/built-up [BU], barren lands [BR], open waters [OW] and Snow/Ice [SI]), each of which provides the prevalence of one land-cover class, expressed as a percentage in a pixel having a resolution of 30 arc-seconds (i.e., 0.00833° resolution).

To reduce computational effort, bioclimatic, DEM, and land cover layers were upsampled to a 0.04167° resolution via the “aggregate” function included in the *terra* package (Hijmans 2024). Among the 12 land-use layers, we excluded *a priori* SI and OW from the HSM modelling, as they represent unsuitable environments for the target species and for insects in general.

To habitat variables, we added a layer of host plants to test whether this covariate could improve the predictive effectiveness of HSM (see Ruzzier et al. 2024, 2025). To this aim, we compiled the host plants list of *L. delicatula* (see Suppl.

material 1: table S1) using information obtained from the European and Mediterranean Plant Protection Organization (EPPO 2015), whose dataset is based on scientific literature, expert assessments, and official reports provided by National Plant Protection Organizations of its member countries. If more than one species belonging to the same genus was known as a host plant, or if congeneric species could be used as vicariant host plant species in areas at risk of invasion or already invaded, the genus was used as the host taxon (e.g., *Acer*). Otherwise, a single species was used as the host plant (e.g., *A. altissima*). For host plants identified at the genus level, all records of each species within the genus were downloaded from GBIF using the “occ_data” function in the *rgbif* R package (Chamberlain et al. 2024). This same approach was applied for host plants at the species level. Data for each host plant taxon were combined into a single layer of georeferenced points using the “as.ppp” function to create a density map via kernel interpolation with the “density.ppp” function; the kernel interpolation radius was estimated with the “bw.ppl”; all functions pertaining to *spatstat* R package (Baddeley and Turner 2005; Baddeley et al. 2005). To reduce potential oversampling, we used the logarithmic transformation of the kernel density maps (representing the quantitative range map of each host plant taxon). To prevent overestimation of each host taxon distribution, we multiplied the logarithmic density layer by the land cover type associated with each taxon habit (e.g., deciduous broadleaf trees) or by the land cover type relevant for economically valuable taxa (e.g., cultivated and managed vegetation); the association between host plant taxa and land cover is indicated in Suppl. material 1: table S1. Finally, we produced an overall host plants layer by extracting the maximum density value found in each grid cell across all host plant layers. Since host plants can locally replace each other, we used the maximum density value rather than summing the density values of all layers to avoid overestimating host plant density. Data on host plant taxa were downloaded from GBIF on September 30, 2024. It should be acknowledged that host plant occurrences are shaped by bioclimatic conditions, and that the kernel density map implicitly incorporates these effects. As a result, bioclimatic influences on the insect species may be indirectly accounted for in the HSM.

To avoid collinearity issues, all environmental covariates used to build the HSM and BSM were subjected to variance inflation factor (VIF) analysis using the “vifcor” function from the *usdm* R package (Naimi et al. 2014). Highly correlated variables, those with a Pearson’s correlation coefficient $|r| > 0.7$, were excluded (Dormann et al. 2013). This analysis was conducted separately within the calibration extents of BSM (broad-range extent: 85°E to 125°E; 0°N to 70°N) and HSM (narrow-range or native extent: 90°E to 125°E; 25°N to 45°N).

None of the land use covariates used in the SDMs were pairwise correlated. Following the VIF analysis, six out of ten bioclimatic variables were retained for the BSM procedure: three related to temperature (BIO2, BIO5, and BIO11) and three related to precipitation (BIO17, BIO18, and BIO19).

Species Distribution Modelling framework

The modelling approach was based on an ensemble procedure (Araújo and New 2007; Guisan et al. 2017). To better assess the influence of environmental variables on *L. delicatula* spatial distribution, bioclimatic and habitat variables (including digital elevation model) were modeled separately in two distinct ensemble models

(HSM and BSM), and their resulting maps combined as a spatial product, following the framework outlined by Ruzzier et al. (2024). We included DEM among the habitat variables to account for local microclimatic variations. This approach is based on the idea that integrating wide-scale (bioclimatic) and narrow-scale (habitat) variables into a single model may result in underestimating the contribution of variables acting at different geographic scales (scenopoetic vs local; *sensu* Hortal et al. 2010, see Franklin 2010). From a probabilistic perspective, this strategy relies on the assumption that bioclimatic suitability, i.e., the probability of finding an occurrence at a given site according to the BSM [$P(\text{BSM})$], represents a necessary but not sufficient condition (a climatic constraint), while habitat suitability, as estimated by the HSM and intrinsically conditioned by bioclimatic factors [$P(\text{HSM}|\text{BSM})$], refines the local probability. Accordingly, the conditional probability is obtained by multiplying the HSM and BSM probability (suitability) maps [$P(\text{BSM}|\text{HSM})=P(\text{BSM})\cdot P(\text{HSM}|\text{BSM})$] (see Grimmer and Storzaker 2001). We acknowledge that the overall suitability map, obtained as the product of the BSM and HSM probability maps, does not represent a formal conditional probability but rather a composite suitability index, since the two models were developed independently. Nevertheless, because HSM is intrinsically conditioned by bioclimatic factors, the composite suitability index can be considered conceptually close to a conditional probability.

When modelling presence-only data, the selection of pseudo-absences (PAs) or background points (BPs) is one of the most critical aspects to address (Barbet-Massin et al. 2012); pseudo-absences should be intended as locations where the species is assumed to be absent, though it was never confirmed through observation, while background points represent randomly sampled locations across the study area where the presence or absence of the species is unknown (Guisan et al. 2017). Sampling PAs or BPs exclusively within a species' native range prevents a proper evaluation of the influence of bioclimatic variables, which primarily operate at broad spatial scales. As a result, the inability to isolate the effects of these bioclimatic factors would hinder the identification of key variables that limit the species' native range and reduce the accuracy of predicting potentially suitable areas beyond that range. Therefore, when working at large spatial scales (e.g., continental or global), it is essential to sample PAs or BPs within the occurrences range and slightly beyond its limits in order to determine whether, and to what extent, bioclimatic variables constrain the species' distribution (see Guisan et al. 2017; Adde et al. 2023). In contrast, variables such as land cover, DEM, and host plants exhibit fine-scale variation and act primarily at the local level, influencing habitat suitability. To assess the effects of these local-scale covariates, PAs or BPs should be selected as close as possible to known presence points (Fournier et al. 2017; Mateo et al. 2019; Adde et al. 2023). This approach minimizes the potential confounding effect of bioclimatic variables on the estimation of habitat-level influences.

Since we empirically observed a relatively high density of occurrences of *L. delicatula* in urban areas, we suspected a possible sampling bias likely due to an easier detection of this species in urban context than in more remote areas (e.g., Beck et al. 2014). To evaluate this observation, we conducted an initial modelling attempt using BPs. As expected, this first output revealed a substantial overestimation of variables associated with anthropogenic contexts, particularly BU (results not shown). To overcome this issue, we decided to use a mixed set of BPs and PAs for HSM calibration, i.e. a random BPs identification combined with PAs identified on the base of a sampling bias map. We first identified an HSM calibration

area (within the narrow-range extent; Suppl. material 2: fig. S1) defined by surfaces where the density of occurrences exceeded 0.001 points/km². Subsequently, we determined a set of PAs, in which the number of PAs equaled the number of occurrences. The allocation of PAs was proportional to the fractional cover of BU within each cell of the calibration area. Additionally, we identified a set of BPs, where the number of BPs equaled four times the number of occurrences within the calibration area. Overall, the total number of PAs + BPs for HSM was five times the number of occurrences (324 PAs + 1296 BPs). For the BSM, we identified BPs across the wide-range extent, setting the total number of BPs at five times the number of occurrences (2010 BPs; Suppl. material 2: fig. S2).

Both HSM and BSM models return a map of suitability in terms of species presence probability. From the spatial product of the two maps of species presence probabilities, we obtained an overall suitability map, which returns the probability of finding the species in each location based on both habitat and bioclimatic covariates (see Ruzzier et al. 2024 for details).

The modelling procedure was performed via the *biomod2* package version 4.2-5-2 (Thuiller et al. 2024). As modelling algorithms, the Artificial Neural Network (ANN), the Flexible Discriminant Analysis (FDA), the Generalized Additive Model (GAM), the Generalized Boosting Model (GBM), Random Forest (RF), the Multiple Adaptive Regression Splines (MARS), and the Maximum Entropy (MAXNET) were used, all under “bigboss” settings (Thuiller et al. 2024). A total of 20 sets of PAs + BPs were used for HSM, and 5 sets of BPs were used for BSM. Given the lack of external data to evaluate the models’ accuracy, a 5-fold cross-validation data-splitting procedure was performed using 80% of the data as the training set with the remaining 20% as the validation set (Ruzzier et al. 2024). Each of the models obtained from both HSM and BSM was validated via two validation metrics: the area under the receiver operating characteristic (ROC) curve (AUC; Hanley and McNeil 1982) and the true skill statistic (TSS, Allouche et al. 2006). From the two metrics, we selected the best 10% models in validation to produce the final ensemble models, one for each metric (Allouche et al. 2006; Mandrekar 2010). Habitat and bioclimatic ensemble models were calculated via the “EMwmean” method in *biomod2* package. To account for the performance of each single model used in building the ensemble model, we weighted its contribution by applying a ‘proportional’ option decay. A three-run permutation procedure was used to assess the importance of each variable included in the ensemble model. The same ensemble model framework was adopted for both the HSM and BSM.

A total of 1,400 models were developed (7 modelling algorithms × 20 sets of (PAs + BPs) × 5 cross-validation runs × 2 validation metrics) for the HSM, and 350 models (7 modelling algorithms × 5 sets of BPs × 5 cross-validation runs × 2 validation metrics) for the BSM.

The HSM and BSM were projected onto the following five geographic extents: 1) native area; 2) global; 3) Eastern and Southeast Asia (ESEA), 4) the United States of America (USA), and 5) Europe. The ESEA projection provides a detailed map of the native range and the closely invaded area (Japan, South Korea and Taiwan). The USA projection provides a map of areas already invaded by *L. delicatula* and those suitable for species establishment; we opted to project the calibrated model over the European territory since this species seems to be present in Spain (iNaturalist record) and because its potential impact on major European agricultural crops, particularly grapevine (*Vitis* spp.) (e.g., Huron et al. 2022; Urban and Leach 2023).

Based on all of the geographic extents, we produced the overall suitability map. Since the output of both HSM and BSM produced suitability maps expressed in terms of probability of occurrence of *L. delicatula* starting from independent datasets, the overall suitability maps were obtained as the product of the HSM and BSM maps. Using the Boyce index (Boyce et al. 2002), we assessed the effectiveness of the overall suitability map in predicting the distribution of *L. delicatula* within the calibration area. We also applied the index to evaluate the predictive performance of the overall suitability maps obtained by projecting the calibrated models onto invaded regions, including the eastern United States, where a major self-sustaining population is established, and South Korea. The Boyce index was used in an exploratory manner for the invasive populations, as these are still expanding and many areas identified as suitable by the model have not yet been colonized. This index measures a model's ability to discriminate among areas of varying suitability by comparing predicted values at presence locations with those expected under a random distribution. Analyses were performed using the *modEvA* package (Barbosa et al. 2013). To detect possible extrapolation effects of the HSM and BSM at the global scale, we used the multivariate environmental similarity surface index (MESS; Elith et al. 2010), implemented in the *dismo* package (Hijmans et al. 2024).

Resistance-Distance Constrained dispersal models

To evaluate the invasion model of *L. delicatula* in the USA and South Korea, where multiple established populations are present, we developed a framework to assess the impact of environmental resistance on the dispersal capacity during the colonization process. This approach was not applied in Japan due to the recent establishment of this pest in that region.

The framework relies on three steps: 1) the estimation of the annual dispersal distance; 2) the identification of the best function defining the resistance surface with respect to species colonization (i.e., species range expansion); 3) the reachable threshold, defined as cumulative cost faced by propagules during the colonization dispersal (this aspect accounts for both the ecological permeability of the environmental matrix and the intrinsic dispersal distance of *L. delicatula*). The invasion model was then used in forecasting potential invasion scenarios in invaded or potentially invadable areas across the world.

Dispersal distance

From a management perspective, besides estimating the annual range expansion, it could also be relevant to assess the magnitude of intrinsic linear dispersal of *L. delicatula*. To this end, from the overall global dataset we used occurrence data from the eastern USA (11,326 records), the only region worldwide where the invasion process is well documented, to estimate the annual range expansion and corresponding expansion rate. These data are consistent with those reported by De Bona et al. (2023).

The annual dispersal distance was estimated by analyzing data from two consecutive years, under the assumption that occurrences were detected immediately following local population establishment. For each point in the dataset corresponding to year i , the closest point in the dataset from year $i+1$ was identified, and the Eu-

clidean distance between them was calculated. Starting from 2015 (when more than one occurrence was available), we selected and bonded among consecutive years all the closest pairwise Euclidean distances. Then, we bootstrapped the overall median of these Euclidean distances, along with its confidence intervals at 95% (Efron and Tibshirani 1993). In addition, we bootstrapped the 99th percentile of the closest pairwise Euclidean distances, and its confidence intervals at 95%. This procedure allowed us to estimate the maximum dispersal distance for *L. delicatula* from one year to another. All points from the year $i+1$, where the value of the closest pairwise Euclidean distances exceeded the 99th percentile, were classified as an event of new introduction due to human-mediated translocation (see “Resistance cost threshold”).

Resistance surfaces

Resistance surfaces are widely used to assess how much environmental features hinder animal dispersal, to both assess the population ecological connectivity (Bani et al. 2015; Lecis et al. 2022, 2024) and to evaluate the colonization processes (Sherpa et al. 2020). To achieve this, we calculated a set of resistance maps as function of the overall suitability map obtained from the SDM framework. We tested two methods to evaluate the resistance encountered by propagules during dispersal: a) resistance defined as the complementary value to suitability (i.e., additive inverse relationship; Zeller et al. 2012; Bani et al. 2018), and b) resistance that varies non-linearly with suitability, following a logistic function (McRae and Beier 2007; Zeller et al. 2012):

$$\text{a) } R = 1 - S$$

$$\text{b) } R = 1 / (1 + \exp(-k * (1 - S - x_0)))$$

where R is the resistance, S is the suitability, k is the steepness and x_0 is the inflection point that determines a change of concavity. In this case we used three sets of values with different values of x_0 (0.25, 0.5, 0.75), while we set k value equal to 15 (Fig. 1). The rationale behind this concept is that colonization begins by prioritizing areas with the lowest resistance, those with the highest suitability (i.e., highest probability of colonization), even if they are geographically farther away but still within the dispersal distance achievable by propagules. Colonization then extends to regions with lower or suboptimal suitability only after these high-suitability areas have been saturated (Lovell et al. 2021). In addition, we assumed that newly colonized cells immediately act as new sources for propagule spread.

We then determined the value of resistance between two neighboring cells of the resistance map, producing a transition matrix, through the function “transition” of the *gdistance* R package (van Etten 2017); in the transition matrix, for a pair of neighboring cells A and B the transition value between them (i.e., the ecological resistance experienced by an organism passing from the cell A to cell B) depends on the resistance values of the two cells and the transition function defining the mathematical relationship between the two cell values; as the transition function we used the reciprocal (i.e., the inverse relationship; Adriaensen et al. 2003; McRae and Beier 2007) of the average value of the two adjacent cells: $f(x) = 1/\text{mean } x$, where x is a vector containing the values of two neighboring cells. The spatial distance between two cells is also considered: for a 3×3 group of cells, the distance between

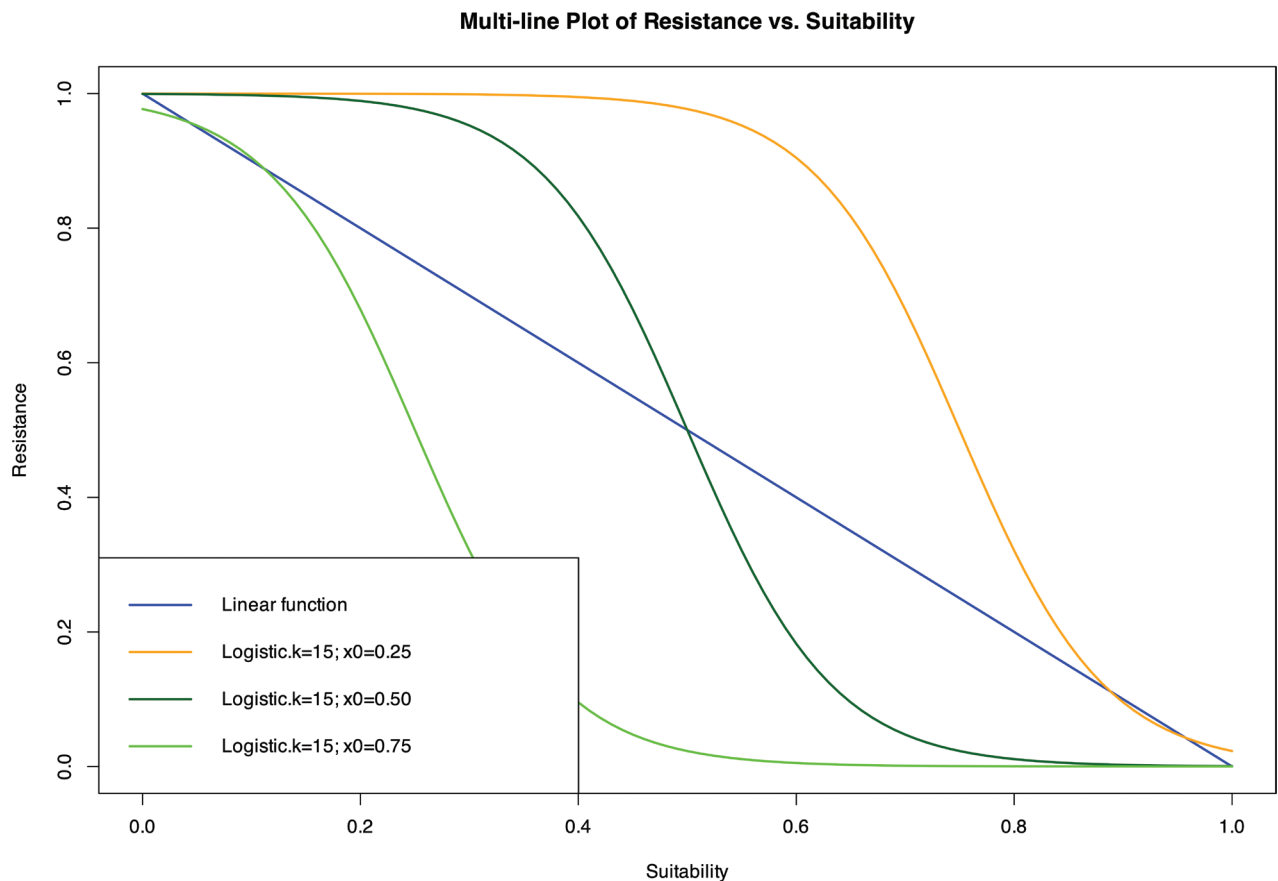


Figure 1. Linear and logistic functions used to calculate resistance surfaces based on environmental suitability.

horizontally and vertically adjacent cells corresponds to the cell resolution, while for diagonally adjacent cells, the distance is equal to the resolution multiplied by the square root of 2; the transition matrix is then corrected to account for geographic distortion, using the function “geoCorrection” implemented in *gdistance*.

Resistance cost threshold

Starting from the colonized cells (just one cell at time 0, i.e., the first documented occurrence), we calculated the cumulative cost derived from the transition matrix for expanding to new cells. To identify the reachable cells by dispersers, we set a cost threshold defining the maximum cumulative cost affordable by them (cost threshold). At time $t+1$, the reachable cells were identified starting from the colonized cell at the time t . Running this procedure from t_0 to t_n , we identified n homocentric annual bands (corresponding to n years), which show the year-by-year range expansion of the species. Starting from the expansion band, we generated annual isochores overlaid on the overall suitability map for the eastern USA, showing the boundaries of areas reached by the population each year. The key point of this step was evaluating the optimal cost threshold, i.e., the threshold providing the best allocation of points within the expansion range, and the corresponding function. This function optimizes the number of points included in the invaded range (i.e., ratio of occurrences within the range to the total occurrences) and the point density (i.e., ratio of occurrences within the range to its area). To this end, we first built a dataset containing all the occurrences that fell within the estimated

dispersal distance between two consecutive years. To be as conservative as possible, we used all occurrences selected based on the 99th percentile of the bootstrapped Euclidean distances (i.e., dispersal distance) from the first colonization point. This approach was intended to include only new occurrences from one year to the next, represented by propagules originating from the first introduction, while excluding occurrences more likely to have a different origin (i.e., those originating from other translocated populations). The assessment was performed for the invaded areas of the eastern USA.

Future invasion scenarios in the USA, South Korea and Japan, and potential invasion scenario in Europe

Based on the invasion model estimated for the eastern USA, we forecasted the USA, South Korea, and Japan invasion scenarios starting from the current distribution of *L. delicatula* in these countries. In addition, given the possible recent detection of *L. delicatula* in Europe, we used the invasion model estimated for the eastern USA to simulate a possible invasion scenario, starting from a) the known locality of species detection (Madrid, Spain); b) potential entry points (relevant ports or airports) located in highly suitable areas for this species (i.e., Milan Malpensa Airport, Italy; Paris Charles de Gaulle Airport, France; Hamburg Port, Germany). All the scenarios were forecasted over a 10-year span.

Results

SDMs performance and effect of covariates

For the HSM, the validation process shows that the top 10% of model scores range from 0.870 to 0.900 according to the AUC of the ROC curve and from 0.585 to 0.697 based on the TSS (Suppl. material 1: table S2). For the BSM, the validation process shows that the top 25% of model scores range from 0.971 to 0.985 according to the AUC of the ROC curve and from 0.855 to 0.898 based on the TSS (Suppl. material 1: table S3). The rationale for selecting the top 10% of 1,400 HSM models and the top 25% of 350 BSM models is a technical decision aimed at optimizing the trade-off between computational time and the representativeness of algorithms within the ensemble model.

The best-performing models (140 out of 1,400 for the HSM and 88 out of 350 for the BSM) were retained to realize the HSM and BSM ensemble models projected over the native range of *L. delicatula*, in the ESEA, USA, Europe, and at global scale. The ensemble modelling process provided the importance of covariates (see Suppl. material 1: tables S4, S5) and the associated response curves for both the HSM and BSM (see Suppl. material 2: figs S3, S4). Habitat suitability was affected mostly by host plants (variable importance HP.max: 0.542), followed by built-up areas (BU: 0.358), cultivated and managed vegetation (CMV: 0.112), herbaceous cover (HERB: 0.079), and elevation (DEM: 0.053). Host plants and built-up areas had a positive effect on the probability of species occurrence, whereas we found a negative effect for cultivated and managed vegetation and herbaceous cover. The elevation graph highlighted that the probability of *L. delicatula* presence was highest between the lowlands and the mid-mountain areas, with an optimum around 750 m asl. Bioclimatic suitability was predominantly influenced by the mean tem-

perature of the coldest quarter (variable importance BIO11: 0.591), with optimal conditions observed around 0 °C (chiefly between −5 and +2 °C). The second most influential variable was the minimum temperature of the warmest month (BIO5: 0.152), indicating optimal conditions above 30 °C. Mean diurnal range (BIO2: 0.100) ranked third in importance, with a temperature range lower than 7.5 °C.

The HSMs in the calibration area, based on ROC and TSS metrics, were highly correlated; the same held true for the BSMs (Pearson's correlation coefficients consistently exceeded 0.99). Habitat suitability and bioclimatic suitability maps, along with their 95% confidence intervals, are provided in Suppl. material 2: figs S5, S6, respectively.

The overall suitability map (Suppl. material 2: fig. S7), obtained from the spatial product of the habitat and bioclimatic suitability maps within the native narrow-range extent, achieved a Boyce index of 1 (Suppl. material 2: fig. S8 for the Boyce graph). Good modelling performance was observed in the overall suitability map, where the occurrences of *L. delicatula* were mostly concentrated in areas with a high probability of species presence (Suppl. material 2: fig. S7). MESS analyses of habitat and bioclimatic variables indicated that extrapolation did not significantly affect the projections (Suppl. material 2: fig. S9a, b). The good forecasting performance of the model projected in the eastern USA (Suppl. material 2: fig. S10) was supported by a Boyce index of 1 (Suppl. material 2: fig. S11). Conversely, for the South Korea projection (Suppl. material 2: fig. S12) the Boyce index was −0.133 (Suppl. material 2: fig. S13), suggesting a strong mismatch between occurrences and suitability.

SDM projections at the global, ESEA, USA and European scale

The projections of HSM and BSM at the global (Suppl. material 2: fig. S14a, b), ESEA (Suppl. material 2: fig. S15a, b), USA (Suppl. material 2: fig. S16a, b), details of eastern USA (Suppl. material 2: figs S17a, b), and European (Suppl. material 2: fig. S18a, b) scales provided the habitat and bioclimatic suitability maps for the four geographic extents, while their product returned the overall suitability maps.

According to the overall suitability map at the global scale (Fig. 2), the most favorable areas for *L. delicatula* within its native range are located in eastern China. The largest continuous suitable region for this species is in central-eastern USA. Japan also exhibits high suitability, encompassing nearly its entire territory. Additional suitable areas are scattered worldwide: while these areas are relatively limited in extent, several are found in Europe, predominantly south of the 55°N latitude.

In particular, ESEA overall suitability map (Fig. 3) which includes the native range in the PR of China, shows multiple suitable areas located along the coastal strip of the country, facing the Yellow Sea and East China Sea. In addition, suitable areas are in the Korean peninsula and Japan, particularly Honshu and Shikoku.

In North America (Fig. 4) the suitable area for *L. delicatula* is mainly located in central-eastern USA, where the main and initial populations are expanding along multiple directions, leading to coalescence with secondary populations originated from human-mediated translocations (see Fig. 5 for details). The primary population has currently established itself in several states, including New Jersey, New York, Pennsylvania, Maryland, Delaware, Washington DC, and Virginia. Additionally, propagules have been detected in Illinois, Indiana, Ohio, and Michigan, specifically in areas exhibiting high habitat suitability for the species.

In Europe (Fig. 6), a vast area suitable for *L. delicatula* extends north of the Alps, spanning the central-northern regions of central-eastern France, Switzerland, the

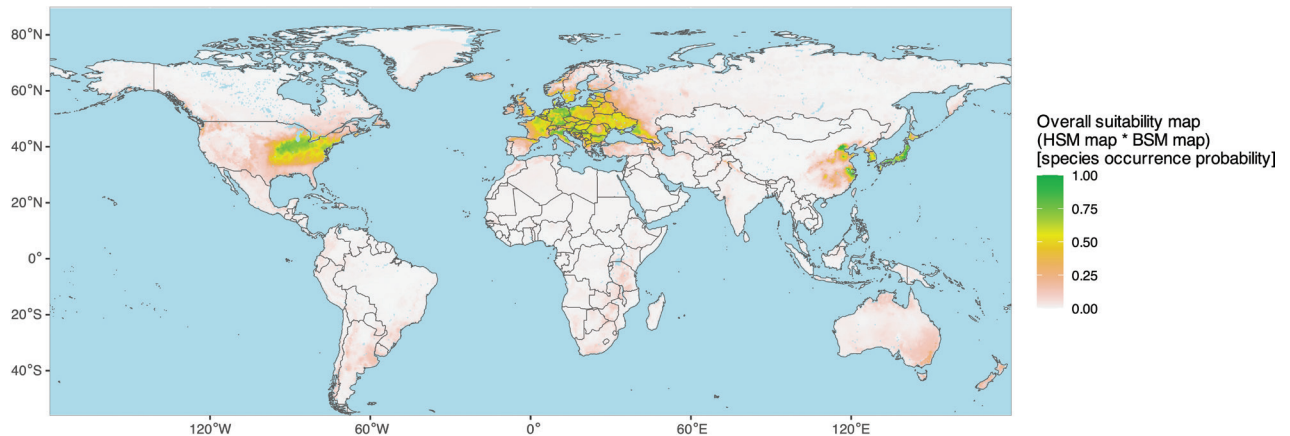


Figure 2. Overall suitability map of *Lycorma delicatula* at a global scale.

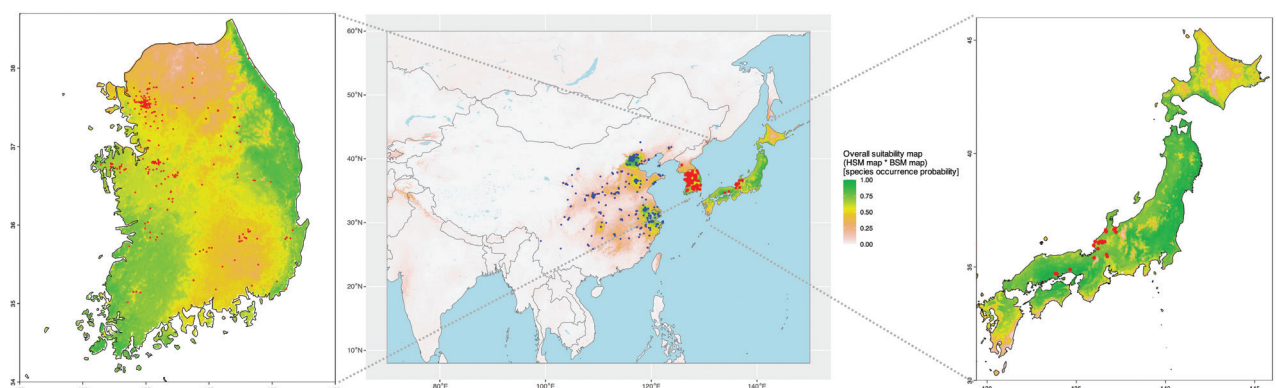


Figure 3. Overall suitability map of *Lycorma delicatula* for Eastern and Southeast Asia (ESEA). In the insets, the detail of the overall suitability in South Korea (left) and Japan (right). Occurrence points: blue: native range; red: invaded range.

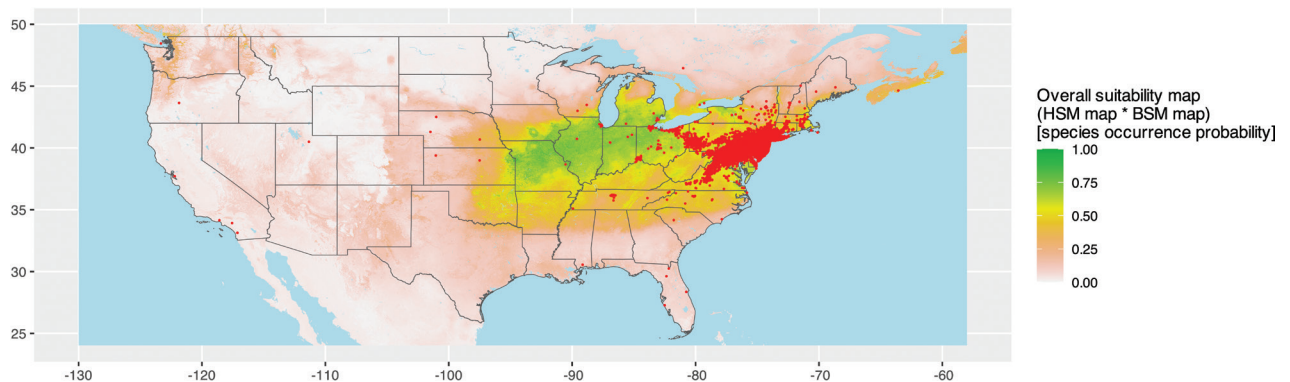


Figure 4. Overall suitability map of *Lycorma delicatula* for USA. Note that the projection extends beyond the political boundaries of the United States, where sporadic occurrences are reported. Red points: *L. delicatula* occurrences.

Benelux countries, and Germany. It reaches the westernmost areas of central-eastern European countries, and extends further north to the Baltic States. South of the Alps, areas suitable for *L. delicatula* are mainly found in a relatively continuous region stretching from the Po Valley in Northern Italy to Slovenia and Croatia farther east.

Multiple large suitable areas are also located along the middle and lower course of the Danube River, spanning Serbia and Hungary to Bulgaria and Romania. Finally, a large suitable area is found from southeastern Ukraine to regions of Russia (Northern Caucasus) bordering the Black Sea and the Sea of Azov.

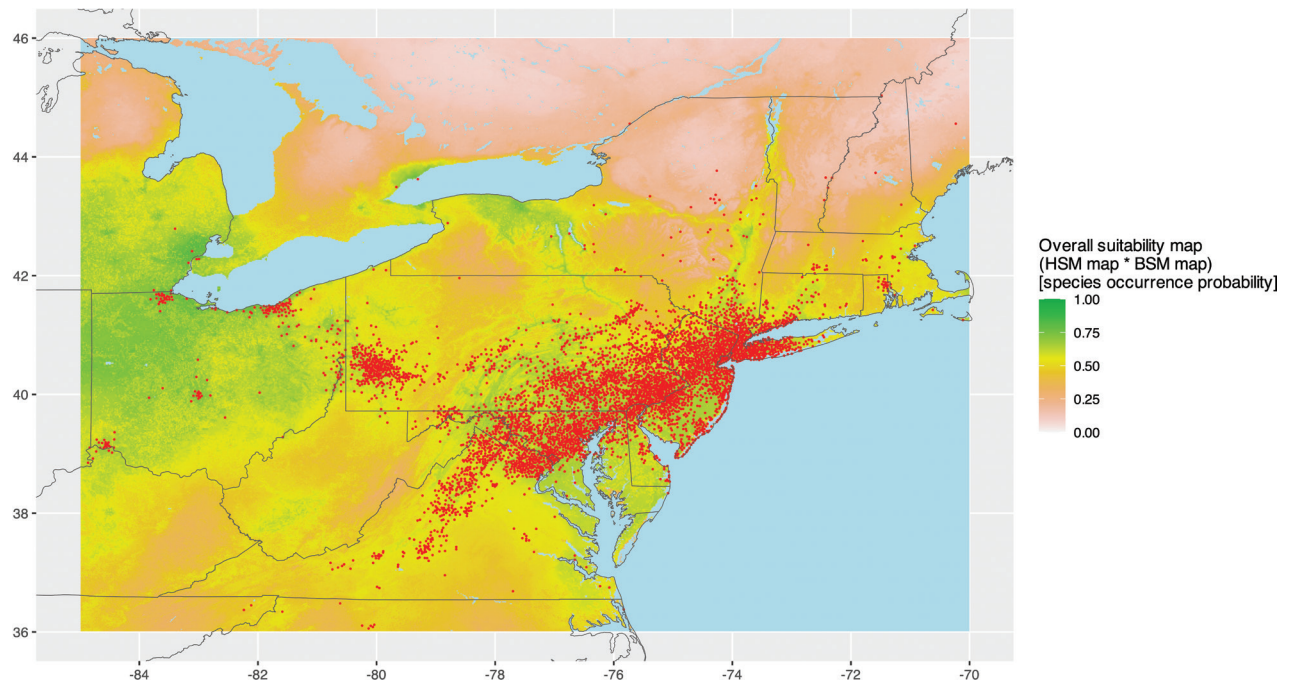


Figure 5. Detail of the overall suitability map of *Lycorma delicatula* for Northeastern US states and adjacent Southeastern Canada. Red points: *L. delicatula* occurrences. Red points: *L. delicatula* occurrences.

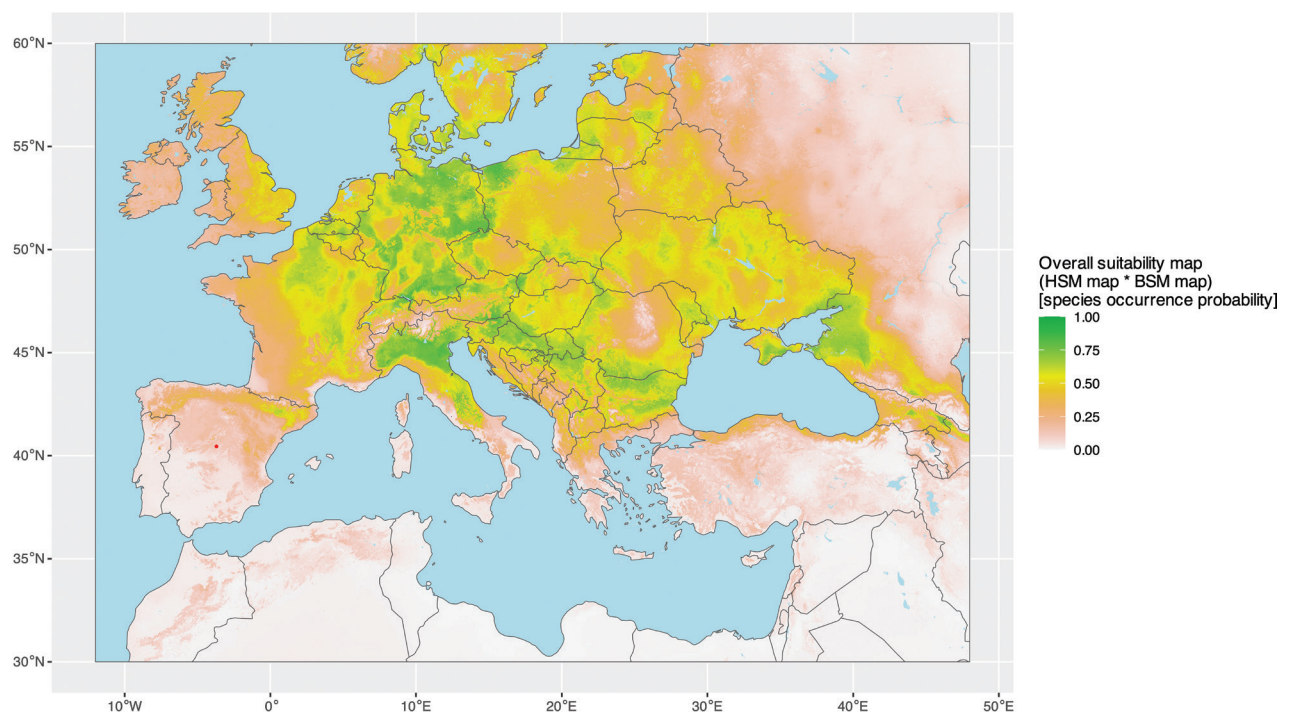


Figure 6. Overall suitability map of *Lycorma delicatula* for Europe. Red point: *L. delicatula* putative occurrence.

Resistance-Distance Constrained Dispersal Model: invasion scenario in USA, South Korea, Japan and Europe

The analysis of *L. delicatula* invasion dynamics was conducted separately for the eastern USA and South Korea to assess consistency between the two regions. However, after an initial exploratory analysis, it emerged that the occurrences in South Korea were highly scattered; this pattern is likely attributable to multiple

human-mediated translocations rather than the natural expansion of *L. delicatula* from the initial entry points. This distribution pattern prevented an accurate estimation of natural invasion dynamics from a specific introduction point. Therefore, the analytical framework for the 10-year invasion dynamics in the USA, Europe, and Japan was developed based on the eastern United States invasion model.

Annual dispersal distance

The frequency distribution of the pairwise shortest distances (Euclidean distances) between occurrences pertaining to consecutive years are represented in Fig. 7. According to bootstrapping estimation, the median of the Euclidean distances was 1,720 m (C.I. 95%: 1680–1766), while the 99th percentile was 25,418 m (C.I. 95%: 18,479–37,038).

Resistance surfaces and cost thresholds

The best function defining the relationship between species suitability and landscape resistance for *L. delicatula* in eastern USA was the logistic function with $x_0 = 0.5$ as midpoint parameter (k was kept fixed to 15), with a cost threshold of 1,200 (i.e., the maximum value of cumulative resistance achievable by propagules while spreading across the invadable area; Table 1).

The species range progression, starting from the first known introduction point, according to the range expansion model (defined by the best function and the best resistance cost threshold), is shown in Fig. 8. The overlap of occurrences in Fig. 8 clearly shows that *L. delicatula* is subject to human-mediated translocations within the invaded range, triggering additional invasion hotspots.

In Table 2, the year-by-year invaded ranges estimated by the range expansion model are provided, according to the best-performing function and resistance

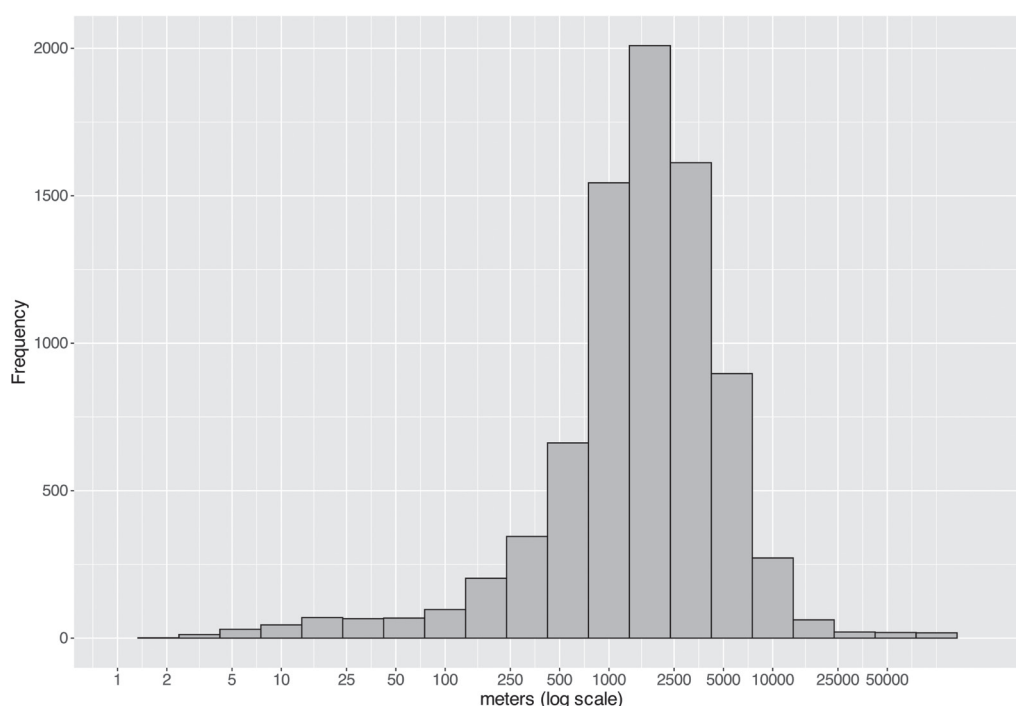


Figure 7. Distribution of frequencies of the pairwise shortest Euclidean distances between occurrences pertaining to consecutive years.

Table 1. Values of attributes obtained from the functions used in assessing the expansion model of *Lycorma delicatula* in the eastern USA. In italics are shown the best thresholds selected by the score for each function and related parameters used in defining the resistance surface. In bold italics: the best threshold associated with the best function.

Functions	Resistance thresholds and spatial attributes	Values of the resistance thresholds and derived spatial attributes					
Linear	Resistance cost threshold	10,500	11,000	<i>11,500</i>	12,000	12,500	13,000
	Invaded range (km ²)	108,418	116,888	125,280	134,093	141,776	149,750
	Point included into the range (%) [A]	78.2	82.3	86.4	89.3	91.2	92.9
	Points/range (points/100km ²) [B]	6.47	6.32	6.19	5.98	5.77	5.57
	Score [A×B]	506.5	520.3	534.1	533.7	526.4	517.2
Logistic: k = 15; x ₀ = 0.25	Resistance cost threshold	17,000	17,250	<i>17,500</i>	17,750	18,000	18,250
	Invaded range (km ²)	133,350	136,314	139,363	142,570	145,342	148,463
	Point included into the range (%) [A]	85.5	86.5	87.9	88.7	89.3	89.9
	Points/range (points/100km ²) [B]	5.77	5.70	5.66	5.58	5.51	5.44
	Score [A×B]	492.2	492.9	497.4	494.8	492.4	488.8
Logistic: k = 15; x ₀ = 0.50	Resistance cost threshold	1,100	1,150	<i>1,200</i>	1,250	1,300	1,350
	Invaded range (km ²)	95,782	98,538	101,283	101,283	101,283	108,114
	Point included into the range (%) [A]	89.6	91.6	93.1	93.9	94.4	94.8
	Points/range (points/100km ²) [B]	5.74	5.87	5.97	6.02	6.05	6.08
	Score [A×B]	537.1	546.0	548.4	545.4	540.0	532.8
Logistic: k = 15; x ₀ = 0.75	Resistance cost threshold	25	30	<i>35</i>	40	45	50
	Invaded range (km ²)	98,368	117,700	140,666	163,061	181,944	201,574
	Point included into the range (%) [A]	68.8	83.8	91.5	93.1	93.4	93.6
	Points/range (points/100km ²) [B]	6.27	6.39	5.83	5.12	4.61	4.17
	Score [A×B]	431.5	534.8	533.6	477.0	430.6	389.8

Table 2. Area invaded by *L. delicatula* in eastern USA from 2015 to 2024 starting from its initial introduction point. The range area was estimated by the range expansion model and refers solely to the year-by-year progression of the populations derived from propagules whose origin is putatively attributed to the initial introduction (it does not include areas occupied by populations believed to have originated after internal translocations mediated by humans).

Year	Invaded area (km ²)
2015	1,797
2016	8,611
2017	21,041
2018	35,724
2019	52,363
2020	72,511
2021	89,480
2022	102,769
2023	115,525
2024	127,721

cost threshold. From just under 2,000 km² colonized in 2015, the invaded area in 2024 had expanded approximately 70-fold, reaching nearly 130,000 km². These areas include only occurrences associated with propagules presumed to originate from the initial introduction (i.e., the area enclosed by the isochores, as illustrated in Fig. 8).

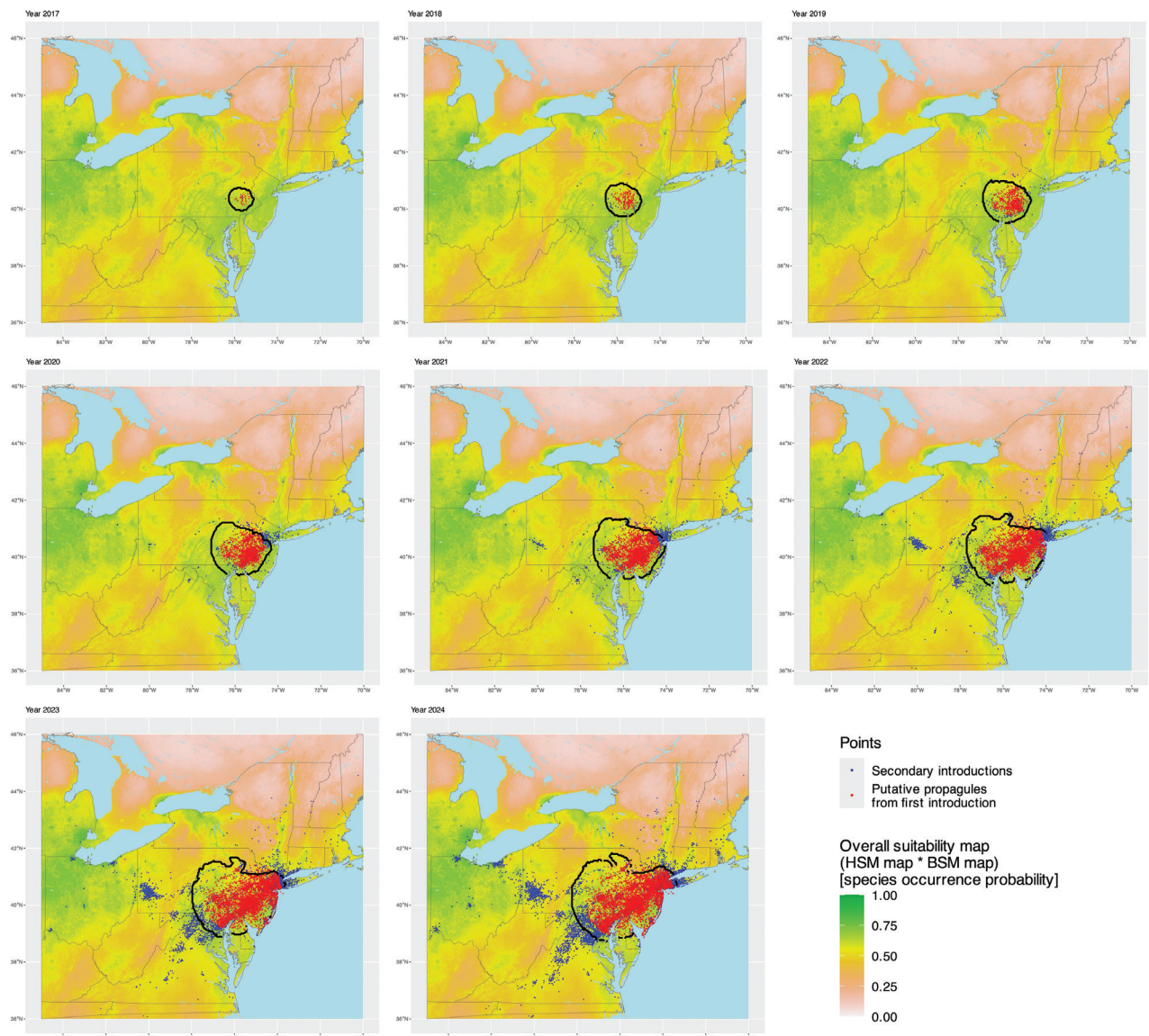


Figure 8. Range expansion model: year-by-year 2017 to 2024 invasion dynamic of *L. delicatula* in eastern USA starting from first introduction. The isochore lines derived from the range expansion model refer solely to the population derived from propagules whose origin is putatively attributed to the initial introduction (it does not include areas occupied by populations believed to have originated from internal translocations mediated by humans). Red points represent the occurrences that are putatively assigned to the population originating from the first introduction event, based on the maximum annual dispersal distance estimated for *L. delicatula* (~25 km).

Future invasion scenarios in the USA, South Korea and Japan, and potential invasion scenario in Europe

The expansion scenarios for *L. delicatula* over the next 10 years in the USA, South Korea and Japan, assessed by the range expansion model and starting from its current distribution, are shown in Figs 9–11, respectively. The European scenario, based on three hypothetical entry points and one iNaturalist recording point for *L. delicatula* (Madrid, Spain), and developed using the eastern USA range expansion model, is illustrated in Fig. 12. This invasion scenario is based on the assumption that population expansion requires prior local establishment. Based on the eastern USA range expansion model, the potential spread of *L. delicatula* in the Iberian Peninsula is unlikely due to the low suitability of the introduction area.

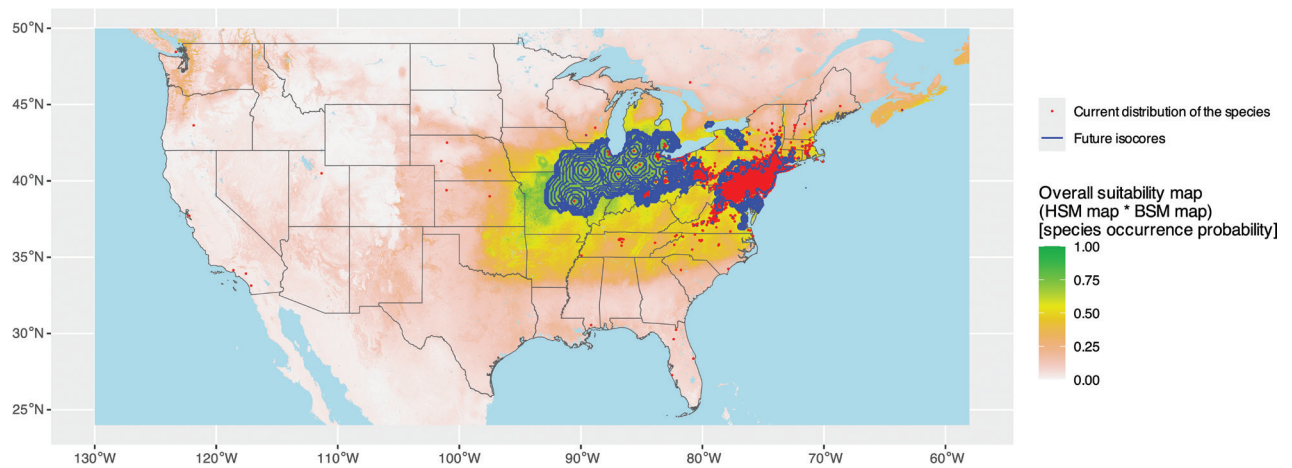


Figure 9. Future invasion scenario of *Lycorma delicatula* in the USA and Southern Canada over the next 10 years, based on the species' current distribution.

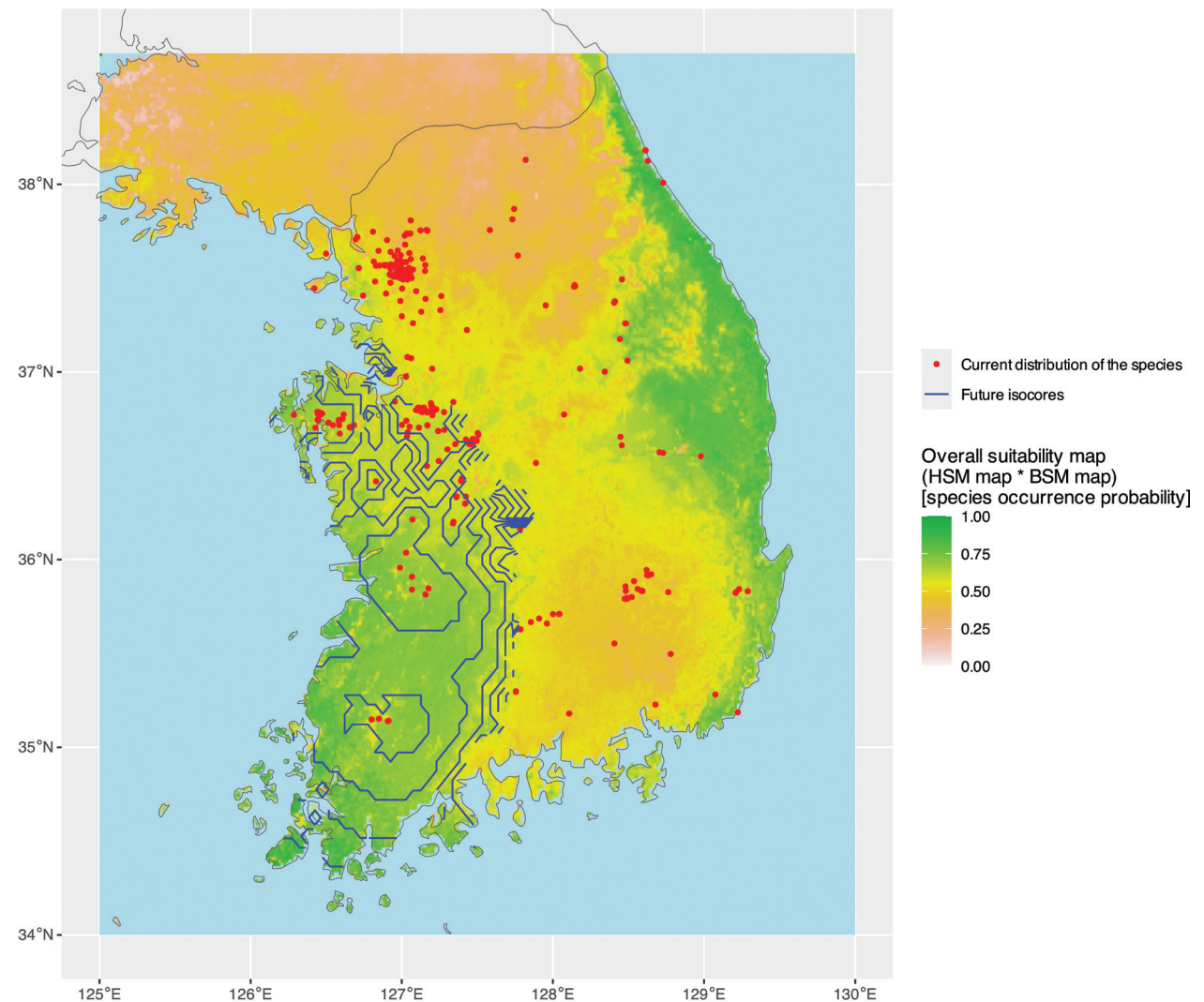


Figure 10. Future invasion scenario of *Lycorma delicatula* in South Korea over the next 10 years, based on the species' current distribution.

All these scenarios should be considered without accounting for potential human-mediated translocations, which could further facilitate the expansion of *L. delicatula* range.

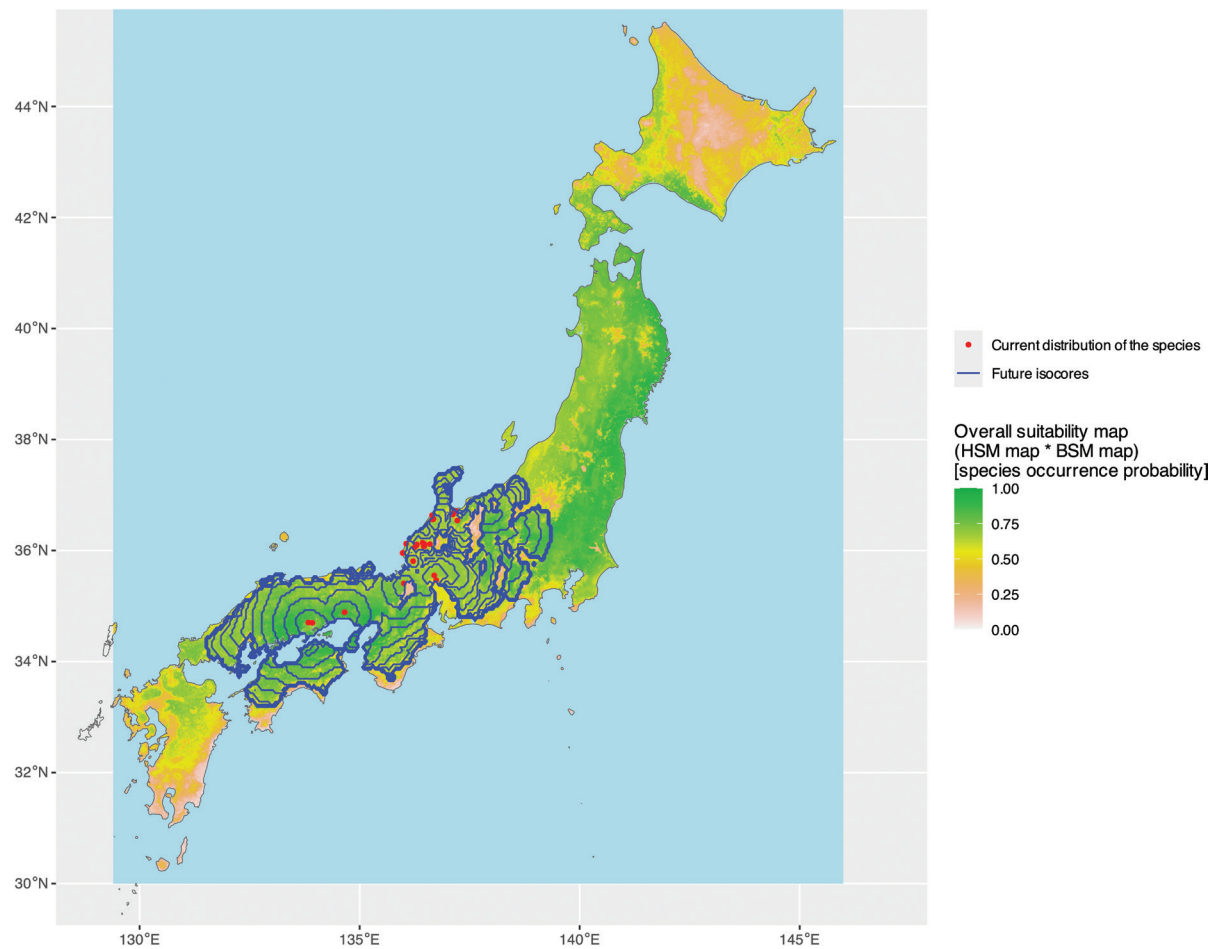


Figure 11. Future invasion scenario of *Lycorma delicatula* in Japan over the next 10 years, based on the species' current distribution.

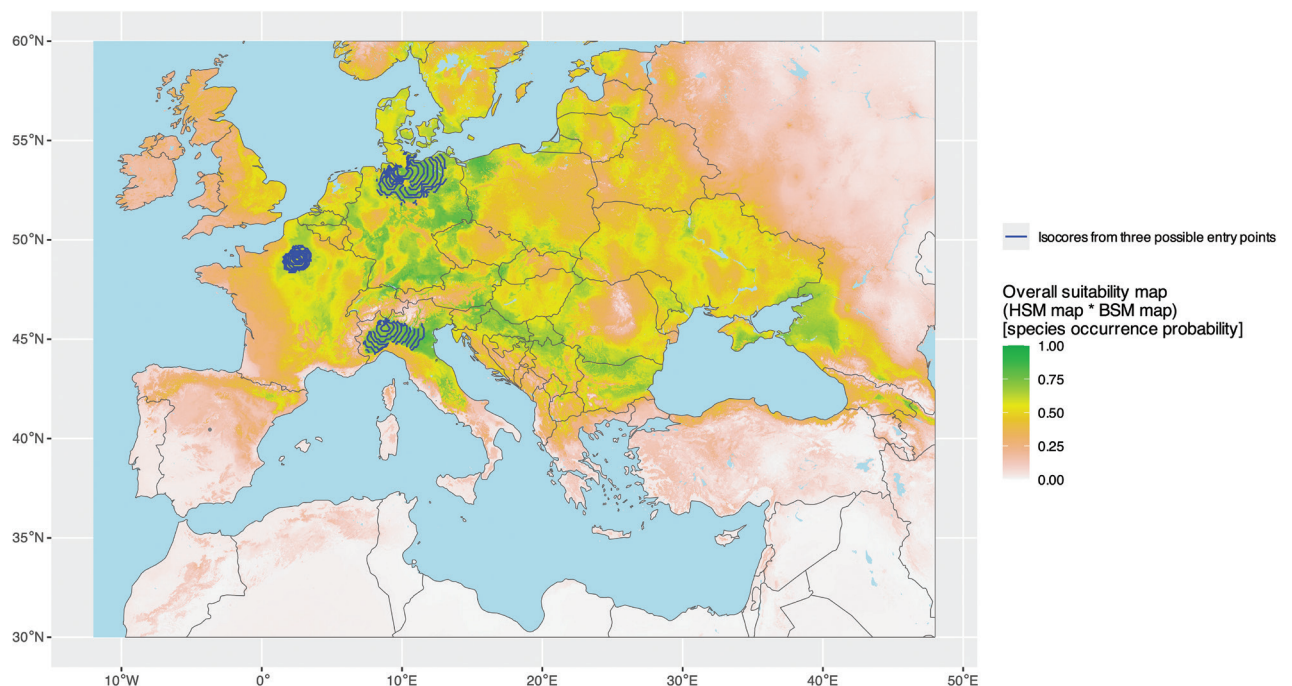


Figure 12. Possible European invasion scenario of *Lycorma delicatula*, assuming three hypothetical entry points 10 years after local population establishment from Milano Malpensa Airport (Italy), Paris Charles de Gaulle Airport (France), and Hamburg Port (Germany). Red points indicate putative occurrences of *L. delicatula*.

Discussion

Species distribution model: comparative evaluation

Although the output of HSM built solely on habitat variables may be partially influenced by bioclimate (host plant taxa and land covers can be affected by climatic conditions to some extent), bioclimatic variables used to build the independent BSM can nonetheless provide a separate contribution to the distribution of *L. delicatula*, distinct from that offered by habitat variables.

Lycorma delicatula seems to be primarily influenced by bioclimatic conditions in its native range. However, within areas that are bioclimatically suitable, habitat availability appears to be a key limiting factor in the species distribution, as indicated by the habitat suitability map.

When considering the overall suitability map, the combined impact of both bioclimatic and habitat factors on the species distribution pattern becomes even more evident. Consequently, it seems unlikely that the species could naturally expand where all its ecological needs are not simultaneously met, as can be observed by the overall suitability map within native range. In addition, within its native range, *L. delicatula* seems unable to expand into nearby areas with suitable habitats and bioclimates when ecological barriers, such as oceans or major mountain ranges, are present.

Built-up areas (BU) emerged as an important variable in the calibration area (i.e., the native range), showing a positive effect on the probability of species presence. This effect is also confirmed by other authors, who have observed a similar influence in areas subject to invasion (Owen et al. 2024; Levine et al. 2025). According to these studies, *L. delicatula* may benefit from the urban environment, particularly due to the presence of host plants used for ornamental purposes, as well as the microclimatic “heat island” effect, which could increase the chances of survival for the species. In addition, the mean temperature of the coldest quarter (BIO11) significantly influences the winter survival of *L. delicatula*, as its eggs require a period of overwintering to break diapause. However, prolonged and extreme cold events can lead to embryo mortality, as previously observed by several authors (Lee et al. 2011, 2014; Keena and Nielsen 2021; Kreitman et al. 2021).

The numerous non-native areas with similar bioclimatic and habitat conditions identified as suitable by our modelling framework can thus be colonized by the species only through human-mediated translocation, due to geographic separation (Ladin et al. 2023).

The adopted approach appears to effectively identify the most suitable areas for *L. delicatula* on a global scale, as all currently invaded areas are classified as suitable or, at least, moderately suitable both in terms of bioclimatic factors and habitat, including host plants (overall probability of species presence ≥ 0.5). For this reason, it can be hypothesized that *L. delicatula* may not be sufficiently plastic to change or expand its ecological niche.

Our results, like several recent studies (Namgung et al. 2020; Wakie et al. 2020; Huron et al. 2022; Chartois et al. 2024; Zhao et al. 2024; Lin and Liao 2025), differ from Jung et al. (2017), who linked *Lycorma delicatula* mainly to tropical and subtropical humid climates. In contrast, most studies, including ours, associate the species with a broader range from humid continental to humid subtropical climates. These differences likely stem from Jung et al. use of the CLIMEX model, while others employed algorithms like Maxent, Random Forest and others.

Our study offers important advancements compared to previous analyses in modeling the distribution of *L. delicatula*. Unlike Namgung et al. (2020), who integrated both bioclimatic and habitat variables (limited to *Vitis vinifera* L. as the host plant) within a single model focused solely on South Korea, our approach models these factors separately, allowing for a more detailed and differentiated assessment. Furthermore, we utilize a composite layer comprising several dozen host plant taxa, in contrast to the single host considered by Namgung et al., and apply an ensemble modeling approach, enhancing prediction robustness. Finally, the allocation of PAs or BPs likely influenced the discrepancies observed between the two studies, as it is well known that modelling techniques based solely on presence data are highly affected by this aspect (as noted by Steen et al. 2024).

Wakie et al. (2020) developed a bioclimatic model incorporating presence data from both the native range and invaded regions, with background points randomly distributed within a large polygon surrounding the occurrence data. Their results are generally consistent with our BSM, except for the native range, where they predict notably lower suitability. Wakie et al. acknowledge that heavy reliance on non-native data in their model likely contributes to the underestimation of suitability in the native range.

Our BSM map largely agrees with that of Huron et al. (2022), which was produced by averaging two different maps: the first based on bioclimatic variables, digital elevation model, forest canopy height, and access to cities, and the second related to the suitability of *Ailanthus altissima* as a host species. The alignment between our BSM map and the overall suitability map by Huron et al. (2022) is largely due to the dominant influence of the bioclimatic covariates in the model that produced the latter map provided by Huron and co-authors.

The suitability map produced by Zhao et al. (2024), based on a Maxent model integrating 19 bioclimatic variables and a digital elevation model, and using occurrence data from both native and invaded regions, largely aligns with our BSM map in terms of global suitability patterns. However, their map generally shows lower suitability values compared to ours. A key limitation of their approach is the random global allocation of background points, which risks placing these points in climatically suitable areas that remain uncolonized due to biogeographic barriers or the recent absence of introductions. This leads to an underestimation of the importance of variables influencing true habitat suitability (see Ruzzier et al. 2025; Steen et al. 2024). Nevertheless, since most suitable regions are already partially or fully invaded by *L. delicatula*, this issue likely had minimal impact on their overall results, as most background points fell within unsuitable areas. Our approach, however, effectively minimizes this caveat.

Chartois et al. (2024) used an ensemble model based on bioclimatic variables to produce a global suitability map largely consistent with our BSM and Zhao et al. (2024). However, while Zhao et al.'s map shows generally lower suitability than ours, Chartois et al.'s map indicates higher suitability in both intensity and geographic extent. Their study properly allocated PAs for bioclimatic modeling but did not exclude regions separated by biogeographic barriers, which may be suitable but uncolonized. The key difference with our BSM likely stems from their use of PAs restricted to the north and south of the presence polygon along a latitudinal gradient, whereas we allocated background points (BPs) across the entire gradient. This comprehensive BP allocation in our model enables a more balanced assessment of bioclimatic effects, while their method may overemphasize conditions

within the presence polygon by assuming it is entirely suitable and areas outside are unsuitable.

The model we developed did not identify the U.S. state of California as a critical area for potential invasion risk, despite some detections of *L. delicatula* reported in literature and databases. We believe these occurrences likely represent adventitious populations, as they have not shown any signs of local range expansion. Such occurrences may have been sustained by commercial transportation (see Jones et al. 2022; Ladin et al. 2023; Montgomery et al. 2023) within a region of low suitability. Conversely, other studies published around the same time (Wakie et al. 2020; Jones et al. 2022; Montgomery et al. 2023) identified California as a suitable area for this pest, based on modelling approaches that included occurrences from populations not yet at equilibrium. However, we argue that calibrating models with occurrences from non-equilibrium populations, such as adventive populations, may distort niche estimation and the influence of covariates, potentially leading to misleading predictions. Similarly, propagules detected in central U.S. states and Florida are in areas of low suitability and thus represent a low invasion risk. The same pattern applies to Canada, where confirmed occurrences occur mostly in areas of low suitability, except for Nova Scotia, the western shores of Lake Ontario, and the northwestern shores of Lake Erie.

Ultimately, Namgung et al. (2020), Huron et al. (2022), Jones et al. (2022), Montgomery et al. (2023), and Chartois et al. (2024) should be credited for acknowledging the importance of incorporating or assessing host plants, albeit through different approaches, when evaluating the suitability for potential colonization by *L. delicatula*.

The analytical framework we have developed is, in our view, capable of providing a more robust predictive capacity, thanks to a series of methodological aspects, many of which represent novel implementations. In particular, the calibration of the model using data from populations in equilibrium within the native range of the species allows for a more realistic assessment of the ecological niche occupied by the species. Furthermore, the criteria adopted to identify BPs and PAs, along with their spatial extent and relationship to occurrence records, play a crucial role in refining the estimation of the influence of environmental covariates. The integration of host plant distributions, combined with high-resolution land cover data, further enhances the estimation of habitat-level suitability, providing a more accurate representation of the ecological requirements of the species. Additionally, the separate implementation of a HSM and a BSM, within a two-step modelling approach, enables a more effective distinction between the effects of local-scale covariates (addressed in the HSM) and those associated with broader-scale ecological processes (addressed in the BSM). Altogether, this modelling strategy leads to an improved explanatory understanding of the distribution of *L. delicatula* within the native range and delivers more effective predictive performance, in line with a niche conservation perspective, in regions outside the native area.

Evaluation of SDM projections

The Boyce index, employed to assess the effectiveness of the SDM calibrated on the native range in predicting the distribution of *L. delicatula* in invaded regions (USA and South Korea), reveals two distinct scenarios. In the USA, although this insect has yet to saturate suitable habitats (with populations still expanding), the

evaluation is highly positive, as a significant proportion of occurrences fall within areas identified as suitable. In contrast, the Boyce index for South Korea indicates that the distribution of occurrences is far from saturating suitable areas and does not exhibit a pattern consistent with natural population expansion. Instead, the occurrences appear highly scattered, likely resulting from multiple introduction events and/or human-mediated translocations, which have initiated or are sustaining various invasion hotspots or may represent adventive populations. Given the recent invasion of Japan by *L. delicatula*, evaluating the accuracy of the model prediction for this region no longer seems appropriate.

Despite the presence of several suitable areas on a global scale, many of these areas, which are currently not invaded, appear to be potentially susceptible to colonization, in agreement with Huron et al. (2022). Several of these areas are characterized by the presence of valuable crops on which this pest could cause a significant economic damage (e.g., grapevine). These areas have a mild climate, with temperatures higher than -11°C during winter (the minimum survival threshold for the insect, as indicated by Lee et al. 2014), and are also human-dominated, with an extensive presence of non-native plants, both invasive and ornamental, used as host plants by *L. delicatula* (Nixon et al. 2023a). These conditions thus greatly support *L. delicatula* populations, creating suitable habitats and facilitating the expansion of this pest by forming invasion corridors, in agreement with Zhang et al. (2023).

Considering the invasion process of *L. delicatula* in ESEA, South Korea is already a largely invaded territory where it can be considered nearly ubiquitous, even at present, with populations ranging from adventive to established. In Taiwan, the risk of invasion is rather limited due to the low suitability across most of the territory, except for the anthropized context of the northern part of the island (e.g., Taipei and the surrounding areas), where adventive populations already exist. In contrast, for Japan, considering the high suitability of much of the territory and the presence of established populations, the risk of invasion appears significant. All these potential risks of invasion should be interpreted in the light of the current climatic and habitat conditions.

Range expansion model and invasion scenarios

Considering both the suitability and the intrinsic dispersal potential of *L. delicatula*, we simulated the insect's range expansion in invaded areas, starting from the current distribution, as well as in potentially invadable areas, over a 10-year period.

Our projections for the United States, where invasive populations are more widespread, identify two major regions at risk of colonization. The first is located east of the Appalachian Mountains, extending toward the Atlantic coast, and appears to be already extensively colonized, with *L. delicatula* having nearly occupied all suitable habitats. The second lies further inland, west of the Appalachians and south of the Great Lakes, where the invasion is ongoing, showing clear directional movement toward the continental interior. Smaller, likely internally relocated populations are already present there, and the model predicts nearly complete colonization of the most suitable areas within the next 10 years. The model also indicates a low likelihood of populations in California, the Central-Western states, and Florida developing into expanding invasive populations.

In South Korea, the 10-year expansion scenario projected from currently colonized areas suggests that potential invasion will likely concentrate along the south-

western coast. Other populations, possibly arising from internal translocations, are unlikely to contribute to further range expansion, including in the Seoul area, despite high occurrence densities recorded there. Given these uncertainties, this invasion pattern should be interpreted with caution, but we deemed it valuable to present this potential scenario in relation to habitat suitability across South Korea.

For Japan, where suitability is high, the 10-year scenario indicates that current populations could rapidly spread through the central and southern regions of Honshu Island. However, the model does not predict full saturation of suitable areas further north within this period, so additional range expansion is still possible.

In Europe, the range expansion simulation emphasizes that successful invasion depends on established populations within medium to highly suitable areas. This is illustrated by the single recorded occurrence in Madrid, Spain, which our model suggests is unlikely to contribute to further spread. Conversely, introductions and establishments in highly suitable areas could lead to rapid expansion, as demonstrated by the three hypothetical entry points included in our simulations.

Pest status perspectives

The findings of this study suggest that, given the limited ecological plasticity and relatively slow expansion rate estimated for *L. delicatula*, the prompt implementation of eradication measures could be particularly effective in eliminating adventive populations. These efforts must be reinforced by stringent measures to prevent the establishment of new invasion hotspots caused by accidental human-mediated dispersal. Additionally, in moderately to highly suitable areas, further efforts are required, including the implementation of effective monitoring protocols and eradication methods as soon as the species is detected.

The damage caused by *L. delicatula* invasion should be assessed considering its potential impact on crops and ornamental plants, derived from its feeding activity and honeydew deposition, especially when it aggregates in huge numbers (Urban and Leach 2023).

As highlighted by the suitability model and the invasion scenarios, a substantial part of the USA remains exposed to the risk of invasion with potentially similar impacts to those observed in other invaded areas, as indicated by Harper et al. (2019), Leach and Leach (2020), Urban (2020), Urban and Leach (2023), and Molfini et al. (2024). Global trade increases the likelihood of *L. delicatula* introductions and associated economic losses in countries with extensive suitable areas for this species, particularly key producers of agricultural and viticultural products, as emphasized by Huron et al. (2022). This scenario appears especially realistic for Europe, given the recent record of this pest in Spain.

Our findings also align with broader invasion ecology principles and with evidence from other invasive herbivores. In many species, bioclimatic conditions determine the broad limits of potential spread, while habitat and host availability act as finer-scale filters. For example, the spread of the Spongy Moth, *Lymantria dispar* (Linnaeus, 1758), across North America depends not only on climatic suitability but also on the distribution of host tree species (Régnière et al. 2012), and the Emerald Ash Borer, *Agrilus planipennis* Fairmaire, 1888, remains tightly constrained by the availability of *Fraxinus* hosts despite suitable climates (Herms and McCullough 2014). Similarly, bark beetle, *Dendroctonus ponderosae* (Hopkins, 1902), dynamics

(illustrate how climate defines physiological boundaries, while local forest composition governs outbreak severity (Bentz et al. 2010). These parallels underline that invasion risk of *L. delicatula* should not be evaluated on climatic suitability alone, but on the combined filtering action of climate, habitat, and dispersal opportunities. Climatic conditions set the physiological limits for survival and development, while the presence and density of suitable host plants affect successful colonization and reproductive output. Local habitat features and composition further regulate population growth and expansion, ultimately shaping the speed and pattern of invasion. Recognizing the interplay of these factors is therefore essential to fully understand the mechanisms underlying *L. delicatula* spread and to accurately assess invasion risk. Our integrated HSM–BSM framework reflects this multi-layered filtering process, emphasizing that climatically suitable areas may not be colonized unless appropriate hosts and habitats are present, and that natural spread remains limited by major geographic barriers unless overcome by human-mediated translocation.

As predicted by our scenario, the introduction of *L. delicatula* into multiple suitable areas across the European subcontinent could trigger a rapid pest expansion, possibly resulting in significant impacts on crop production. Countries like France, Italy, and Germany, among the world’s largest wine producers, are particularly vulnerable to the invasion risk of *L. delicatula*, as a significant portion of their territory is highly suitable for this pest. The accidental introduction of *L. delicatula* in these regions could indeed cause severe damage to the wine production sector, leading to substantial losses as documented in Pennsylvania, USA (Leach and Leach 2020), where, in 2018, up to 90% of grapes were lost despite the use of insecticides (Urban 2020). The potential impact on the fruit production sector should also not be underestimated. However, these impacts may depend on the features of the agroecosystem in question, including management strategies, as discussed in Nixon et al. (2023b) and Urban and Leach (2023).

Conclusions

The SDM and the spread model implemented in this study represent valuable tools for managing *L. delicatula* and invasive species more broadly, as they enable the precise identification of areas at highest risk of invasion, including both colonization and expansion phases. This would support the development and implementation of early surveillance and targeted monitoring strategies, optimizing resource allocation and enhancing the effectiveness of interventions, while reducing unnecessary costs in low-risk areas. Moreover, mapping environmental suitability is crucial for effectively planning potential introductions of biological control agents, by identifying areas where such actions are most likely to succeed. The outputs of these models also provide a solid basis to support political and management decisions, offering useful insights for defining quarantine zones, regulating the movement of goods, or launching outreach and awareness campaigns for local communities. Looking ahead, integrating these models with socio-economic data, such as transportation flows or commercial activities, could further improve predictive accuracy by more precisely identifying human-mediated dispersal routes and potential entry points. Finally, extending these approaches to future climate scenarios would allow anticipation of invasion dynamics over the medium to long term, enabling proactive and adaptive planning of management strategies.

Acknowledgements

The authors express their sincere gratitude to the three reviewers and the editor for their thorough and expert evaluation, which has substantially enhanced the quality and clarity of the manuscript.

Additional information

Conflict of interest

The authors have declared that no competing interests exist.

Ethical statement

No ethical statement was reported.

Use of AI

No use of AI was reported.

Funding

Funder: Project funded under the National Recovery and Resilience Plan (NRRP), Mission 4 Component 2 Investment 1.4 – Call for tender No. 3138 of 16 December 2021, rectified by Decree n.3175 of 18 December 2021 of the Italian Ministry of University and Research funded by the European Union – NextGenerationEU. Award Number: Project title “National Biodiversity Future Center – NBFC”, Project code CN_00000033, Concession Decree No. 1034 of 17 June 2022 adopted by the Italian Ministry of University and Research, CUP: F83C22000730006, CUP: H43C22000530001.

Author contributions

Conceptualization, E.R., D.S., A.P. and L.B.; methodology and formal analysis, E.R., P.T. and L.B.; data curation and validation, E.R. and D.S.; writing–original draft preparation, E.R. D.S., P.T. and L.B.; writing–review and editing, E.R., P.T., D.S., V.O., A.G., A.P. and L.B.; supervision, E.R. and L.B.; Funding acquisition: E.R., A.G., O.D. and L.B.

Author ORCIDs

Enrico Ruzzier  <https://orcid.org/0000-0003-1020-1247>

Davide Scaccini  <https://orcid.org/0000-0002-6850-7911>

Pietro Tirozzi  <https://orcid.org/0000-0001-5854-6864>

Valerio Orioli  <https://orcid.org/0000-0002-5777-0255>

Olivia Dondina  <https://orcid.org/0000-0001-8097-1971>

Andrea Di Giulio  <https://orcid.org/0000-0003-0508-0751>

Alberto Pozzebon  <https://orcid.org/0000-0002-2445-7211>

Luciano Bani  <https://orcid.org/0000-0001-5795-9499>

Data availability

All of the data that support the findings of this study are available in the main text or Supplementary Information.

References

Adde A, Rey P-L, Brun P, Külling N, Fopp F, Altermatt F, Broennimann O, Lehmann A, Petitpierre B, Zimmermann NE, Pellissier L, Guisan A (2023) N-SDM: A high-performance computing

- pipeline for nested species distribution modelling. *Ecography* 2023(6): e06540. <https://doi.org/10.1111/ecog.06540>
- Adriaensen F, Chardon JP, De Blust G, Swinnen E, Villalba S, Gulinck H, Matthysen E (2003) The application of 'least-cost' modelling as a functional landscape model. *Landscape and Urban Planning* 64(4): 233–247. [https://doi.org/10.1016/S0169-2046\(02\)00242-6](https://doi.org/10.1016/S0169-2046(02)00242-6)
- Allouche O, Tsoar A, Kadmon R (2006) Assessing the accuracy of species distribution models: Prevalence, kappa and the true skill statistic (TSS). *Journal of Applied Ecology* 43(6): 1223–1232. <https://doi.org/10.1111/j.1365-2664.2006.01214.x>
- Araújo MB, New M (2007) Ensemble forecasting of species distributions. *Trends in Ecology & Evolution* 22(1): 42–47. <https://doi.org/10.1016/j.tree.2006.09.010>
- Baddeley A, Turner R (2005) spatstat: An R package for analysing spatial point patterns. *Journal of Statistical Software* 12(6). <https://doi.org/10.18637/jss.v012.i06>
- Baddeley A, Rubak E, Turner R (2005) *Spatial Point Patterns: Methodology and Applications with R*. CRC Press, Boca Raton, USA, 826 pp.
- Bani L, Pisa G, Luppi M, Spilotros G, Fabbri E, Randi E, Orioli V (2015) Ecological connectivity assessment in a strongly structured Fire Salamander (*Salamandra salamandra*) population. *Ecology and Evolution* 5(16): 3472–3485. <https://doi.org/10.1002/ece3.1617>
- Bani L, Orioli V, Pisa G, Dondina O, Fagiani S, Fabbri E, Sozio G (2018) Landscape determinants of genetic differentiation, inbreeding, and genetic drift in the Hazel Dormouse (*Muscardinus avelanarius*). *Conservation Genetics* 19(2): 283–296. <https://doi.org/10.1007/s10592-017-0999-6>
- Barbet-Massin M, Jiguet F, Albert CH, Thuiller W (2012) Selecting pseudo-absences for species distribution models: how, where and how many? *Methods in Ecology and Evolution* 3 (2): 327–338. <https://doi.org/10.1111/j.2041-210X.2011.00172.x>
- Barbosa AM, Real R, Munoz AR, Brown JA (2013) New measures for assessing model equilibrium and prediction mismatch in species distribution models. *Diversity & Distributions* 19(10): 1333–1338. <https://doi.org/10.1111/ddi.12100>
- Beck J, Böller M, Erhardt A, Schwanghart W (2014) Spatial bias in the GBIF database and its effect on modeling species' geographic distributions. *Ecological Informatics* 19: 10–15. <https://doi.org/10.1016/j.ecoinf.2013.11.002>
- Bentz BJ, Régnière J, Fettig CJ, Hansen EM, Hayes JL, Hicke JA, Kelsey RG, Negrón JF, Seybold SJ (2010) Climate change and bark beetles of the western United States and Canada: Direct and indirect effects. *Bioscience* 60(8): 602–613. <https://doi.org/10.1525/bio.2010.60.8.6>
- Boyce MS, Vernier PR, Nielsen SE, Schmiegelow FKA (2002) Evaluating resource selection functions. *Ecological Modelling* 157(2–3): 281–300. [https://doi.org/10.1016/S0304-3800\(02\)00200-4](https://doi.org/10.1016/S0304-3800(02)00200-4)
- CABI (2020) *Lycorma delicatula* (Spotted Lanternfly). <https://www.cabidigitallibrary.org/doi/full/10.1079/cabicompendium.110524> [Accessed on 2024-12-11]
- Chamberlain S, Oldoni D, Barve V, Desmet P, Geffert L, Mcglinn D, Ram K, Walle J (2024) rgbif: Interface to the global biodiversity information facility. R package version 3.7.9. <https://CRAN.R-project.org/package=rgbif>
- Chartois M, Fried G, Rossi JP (2024) Climate and host plant availability are favourable to the establishment of *Lycorma delicatula* in Europe. *Agricultural and Forest Entomology* 27(2): 316–328. <https://doi.org/10.1111/afe.12665>
- Dang YQ, Zhang YL, Wang XY, Xin B, Quinn NF, Duan JJ (2021) Retrospective analysis of factors affecting the distribution of an invasive wood-boring insect using native range data: The importance of host plants. *Journal of Pest Science* 94(3): 981–990. <https://doi.org/10.1007/s10340-020-01308-5>
- Dara SK, Barringer L, Arthurs SP (2015) *Lycorma delicatula* (Hemiptera: Fulgoridae): a new invasive pest in the United States. *Journal of Integrated Pest Management* 6(1): 1–6. <https://doi.org/10.1093/jipm/pmv021>

- De Bona S, Barringer L, Kurtz P, Losiewicz J, Parra GR, Helmus MR (2023) lydemapr: An R package to track the spread of the invasive Spotted Lanternfly (*Lycorma delicatula* White, 1845) (Hemiptera, Fulgoridae) in the United States. *NeoBiota* 86: 151–168. <https://doi.org/10.3897/neobiota.86.101471>
- Dormann CF, Elith J, Bacher S, Buchmann C, Carl G, Carré G, García Márquez JR, Gruber B, Lafourcade B, Leitão PJ, Münkemüller T, McClean C, Osborne PE, Reineking B, Schröder B, Skidmore AK, Zurell D, Lautenbach S (2013) Collinearity: A review of methods to deal with it and a simulation study evaluating their performance. *Ecography* 36(1): 27–46. <https://doi.org/10.1111/j.1600-0587.2012.07348.x>
- Efron B, Tibshirani RJ (1993) *An Introduction to the Bootstrap*. Chapman & Hall, New York, 436 pp. <https://doi.org/10.1007/978-1-4899-4541-9>
- Elith J (2017) Predicting distributions of invasive species. In: Venette RC (Ed.) *Invasive Species: Risk Assessment and Management*. Cambridge University Press, Cambridge, 151–175. <https://doi.org/10.1017/9781139019606.006>
- Elith J, Kearney M, Phillips S (2010) The art of modelling range-shifting species. *Methods in Ecology and Evolution* 1(4): 330–342. <https://doi.org/10.1111/j.2041-210X.2010.00036.x>
- Elsensohn JE, Nixon LJ, Kloos A, Leskey TC (2023) Development and survivorship of *Lycorma delicatula* (Hemiptera: Fulgoridae) on cultivated and native *Vitis* spp. (Vitales: Vitaceae) of the Eastern United States. *Journal of Economic Entomology* 116(6): 2207–2211. <https://doi.org/10.1093/jee/toad198>
- EPPO (2015) *Lycorma delicatula* (LYCMDE). <https://gd.eppo.int/taxon/LYCMDE> [Accessed on 2024-11-15]
- EPPO (2023) Rapid Pest Risk Analysis (PRA) for *Lycorma delicatula*. <https://pra.eppo.int/pra/7507871c-76c8-49f9-af2c-904911fc8e91> [Accessed on 2025-03-23]
- Fournier A, Barbet-Massin M, Rome Q, Courchamp F (2017) Predicting species distribution combining multi-scale drivers. *Global Ecology and Conservation* 12: e00367. <https://doi.org/10.1016/j.gecco.2017.11.002>
- Franklin J (2010) *Mapping Species Distribution: Spatial Inference and Prediction*. Cambridge University Press, Cambridge, 340 pp. <https://doi.org/10.1017/CBO9780511810602>
- Grimmett GR, Stirzaker DR (2001) *Probability and Random Processes* (3rd ed.). Oxford University Press, New York, USA, 608 pp.
- Guisan A, Thuiller W, Zimmermann NE (2017) *Habitat Suitability and Distribution Models: With Applications in R*. Cambridge University Press, Cambridge, UK, 514 pp. <https://doi.org/10.1017/9781139028271>
- Hanley JA, McNeil BJ (1982) The meaning and use of the area under a receiver operating characteristic (ROC) curve. *Radiology* 143(1): 29–36. <https://doi.org/10.1148/radiology.143.1.7063747>
- Harner AD, Leach HL, Briggs L, Centinari M (2022) Prolonged phloem feeding by the Spotted Lanternfly, an invasive planthopper, alters resource allocation and inhibits gas exchange in grapevines. *Plant Direct* 6(10): e452. <https://doi.org/10.1002/pld3.452>
- Harper JK, Stone W, Kelsey TW, Kime LF (2019) Potential Economic Impact of the Spotted Lanternfly on Agriculture and Forestry in Pennsylvania. Report 84, Center for Rural Pennsylvania, Harrisburg, 84 pp.
- Herms DA, McCullough DG (2014) Emerald Ash Borer invasion of North America: History, biology, ecology, impacts, and management. *Annual Review of Entomology* 59: 13–30. <https://doi.org/10.1146/annurev-ento-011613-162051>
- Hijmans R (2024) terra: Spatial Data Analysis. R package version 1.7-78. <https://CRAN.R-project.org/package=terra>
- Hijmans R, Phillips S, Leathwick J, Elith J (2024) dismo: Species Distribution Modeling. R package version 1.3-16. <https://CRAN.R-project.org/package=dismo>
- Hoover K, Iavorivska L, Lavelly EK, Uyi O, Walsh B, Swackhamer E, Johnson A, Eissenstat DM (2023) Effects of long-term feeding by Spotted Lanternfly (Hemiptera: Fulgoridae) on ecophysio-

- ology of common hardwood host trees. *Environmental Entomology* 52(5): 888–899. <https://doi.org/10.1093/ee/nvad084>
- Hortal J, Roura-Pascual N, Sanders NJ, Rahbek C (2010) Understanding (insect) species distributions across spatial scales. *Ecography* 33(1): 51–53. <https://doi.org/10.1111/j.1600-0587.2009.06428.x>
- Huron NA, Behm JE, Helmus MR (2022) Paninvasion severity assessment of a US grape pest to disrupt the global wine market. *Communications Biology* 5(1): e655. <https://doi.org/10.1038/s42003-022-03580-w>
- Jones C, Skrip MM, Seliger BJ, Jones S, Wakie T, Takeuchi Y, Petras V, Petrasova A, Meentemeyer RK (2022) Spotted Lanternfly predicted to establish in California by 2033 without preventative management. *Communications Biology* 5(5): e558. <https://doi.org/10.1038/s42003-022-03447-0>
- Jung JM, Jung S, Byeon DH, Lee WH (2017) Model-based prediction of potential distribution of the invasive insect pest, Spotted Lanternfly *Lycorma delicatula* (Hemiptera: Fulgoridae), by using CLIMEX. *Journal of Asia-Pacific Biodiversity* 10(4): 532–538. <https://doi.org/10.1016/j.japb.2017.07.001>
- Jung M, Kho JW, Gook DH, Lee YS, Lee DH (2022) Dispersal and oviposition patterns of *Lycorma delicatula* (Hemiptera: Fulgoridae) during the oviposition period in *Ailanthus altissima* (Simaroubaceae). *Scientific Reports* 12(1): e9972. <https://doi.org/10.1038/s41598-022-14264-0>
- Keena MA, Nielsen AL (2021) Comparison of the hatch of newly laid *Lycorma delicatula* (Hemiptera: Fulgoridae) eggs from the United States after exposure to different temperatures and durations of low temperature. *Environmental Entomology* 50(2): 410–417. <https://doi.org/10.1093/ee/nvaa177>
- Kindt R, Coe R (2005) Tree Diversity Analysis. A Manual and Software for common Statistical Methods for Ecological and Biodiversity Studies. World Agroforestry Centre (ICRAF), Nairobi, 196 pp.
- Kreitman D, Keena MA, Nielsen AL, Hamilton G (2021) Effects of temperature on development and survival of nymphal *Lycorma delicatula* (Hemiptera: Fulgoridae). *Environmental Entomology* 50(1): 183–191. <https://doi.org/10.1093/ee/nvaa155>
- Ladin ZS, Eggen DA, Trammell TL, D’Amico V (2023) Human-mediated dispersal drives the spread of the Spotted Lanternfly (*Lycorma delicatula*). *Scientific Reports* 13(1): e1098. <https://doi.org/10.1038/s41598-022-25989-3>
- Leach A, Leach H (2020) Characterizing the spatial distributions of Spotted Lanternfly (Hemiptera: Fulgoridae) in Pennsylvania vineyards. *Scientific Reports* 10(1): e20588. <https://doi.org/10.1038/s41598-020-77461-9>
- Lecis R, Dondina O, Orioli V, Biosi D, Canu A, Fabbri G, Iacolina L, Cossu A, Bani L, Apollonio M, Scandura M (2022) Main roads and land cover shaped the genetic structure of a Mediterranean island Wild Boar population. *Ecology and Evolution* 12(4): e8804. <https://doi.org/10.1002/ece3.8804>
- Lecis R, Chirichella R, Dondina O, Orioli V, Azzu S, Canu A, Torretta E, Bani L, Apollonio M, Scandura M (2024) Same landscape, different connectivity: Contrasting patterns of gene flow in two sympatric ungulates in a mountain area. *European Journal of Wildlife Research* 70(3): 1–42. <https://doi.org/10.1007/s10344-024-01796-1>
- Lee JS, Kim IK, Koh SH, Cho SJ, Jang SJ, Pyo, Choi WI (2011) Impact of minimum winter temperature on *Lycorma delicatula* (Hemiptera: Fulgoridae) egg mortality. *Journal of Asia-Pacific Entomology* 14(1): 123–125. <https://doi.org/10.1016/j.aspen.2010.09.004>
- Lee YS, Jang MJ, Kim JY, Kim JR (2014) The effect of winter temperature on the survival of lantern fly, *Lycorma delicatula* (Hemiptera: Fulgoridae) eggs. *Korean Journal of Applied Entomology* 53(3): 311–315. <https://doi.org/10.5656/KSAE.2014.07.0.034>
- Lee DH, Park YL, Leskey TC (2019) A review of biology and management of *Lycorma delicatula* (Hemiptera: Fulgoridae), an emerging global invasive species. *Journal of Asia-Pacific Entomology* 22(2): 589–596. <https://doi.org/10.1016/j.aspen.2019.03.004>
- Levine BA, Moffitt A, Mendez R III (2025) Invasive Spotted Lanternflies (*Lycorma delicatula*) are larger in more urban areas. *Integrative and Comparative Biology* 65(2): 276–284. <https://doi.org/10.1093/icb/ica013>

- Lin YS, Liao JR (2025) Assessing current distribution and climate-driven potential invasion areas of *Lycorma delicatula*, with a focus on Taiwan. *Biological Invasions* 27(7): e161. <https://doi.org/10.1007/s10530-025-03620-6>
- Lovell RS, Blackburn TM, Dyer EE, Pigot AL (2021) Environmental resistance predicts the spread of alien species. *Nature Ecology & Evolution* 5(3): 322–329. <https://doi.org/10.1038/s41559-020-01376-x>
- Mandrekar JN (2010) Receiver operating characteristic curve in diagnostic test assessment. *Journal of Thoracic Oncology : Official Publication of the International Association for the Study of Lung Cancer* 5(9): 1315–1316. <https://doi.org/10.1097/JTO.0b013e3181ec173d>
- Mateo RG, Gastón A, Aroca-Fernández MJ, Broennimann O, Guisan A, Saura S, García-Viñas JI (2019) Hierarchical species distribution models in support of vegetation conservation at the landscape scale. *Journal of Vegetation Science* 30 (2): 386–396. <https://doi.org/10.1111/jvs.12726>
- McRae BH, Beier P (2007) Circuit theory predicts gene flow in plant and animal populations. *Proceedings of the National Academy of Sciences of the United States of America* 104(50): 19885–19890. <https://doi.org/10.1073/pnas.0706568104>
- Molfini M, West M, Gómez-Marco F, Torres JB, Hoddle M (2024) Is *Lycorma delicatula* (Hemiptera: Fulgoridae) a blooming threat to citrus? *Journal of Economic Entomology* 117(5): 2194–2198. <https://doi.org/10.1093/jee/toae197>
- Montgomery K, Walden-Schreiner C, Saffer A, Jones C, Seliger BJ, Worm T, Tateosian L, Shukunobe M, Kumar S, Meentemeyer RK (2023) Forecasting global spread of invasive pests and pathogens through international trade. *Ecosphere* 14(12): e4740. <https://doi.org/10.1002/ecs2.4740>
- Naimi B, Hamm NAS, Groen TA, Skidmore AK, Toxopeus AG (2014) Where is positional uncertainty a problem for species distribution modelling? *Ecography* 37(2): 191–203. <https://doi.org/10.1111/j.1600-0587.2013.00205.x>
- Namgung H, Kim MJ, Baek S, Lee JH, Kim H (2020) Predicting potential current distribution of *Lycorma delicatula* (Hemiptera: Fulgoridae) using MaxEnt model in South Korea. *Journal of Asia-Pacific Entomology* 23(2): 291–297. <https://doi.org/10.1016/j.aspen.2020.01.009>
- Nixon LJ, Jones S, Dechaine AC, Ludwick D, Hickin M, Sullivan L, Elsensohn JA, Gould J, Keena M, Kuhar T, Pfeifer DG, Leskey TC (2022) Development of rearing methodology for the invasive Spotted Lanternfly, *Lycorma delicatula* (Hemiptera: Fulgoridae). *Frontiers in Insect Science* 2: e1025193. <https://doi.org/10.3389/finsc.2022.1025193>
- Nixon LJ, Barnes C, Leskey TC (2023a) Assessing acceptability of wild and cultivated hosts of *Lycorma delicatula* (Hemiptera: Fulgoridae) under semifield conditions. *Environmental Entomology* 52(5): 879–887. <https://doi.org/10.1093/ee/nvad078>
- Nixon LJ, Barnes C, Wilson C, Rugh A, Carper L, Leskey TC, Tang L (2023b) Short-and long-term effects of season-long infestation of *Lycorma delicatula* (Hemiptera: Fulgoridae) on young apple (*Malus domestica*) and peach (*Prunus persica*) trees. *Journal of Economic Entomology* 116(6): 2062–2069. <https://doi.org/10.1093/jee/toad187>
- Owen HL, Meng F, Winchell KM (2024) Urbanization and environmental variation drive phenological changes in the Spotted Lanternfly, *Lycorma delicatula* (Hemiptera: Fulgoridae). *Biological Journal of the Linnean Society. Linnean Society of London* 143(4): blae099. <https://doi.org/10.1093/biolinnean/blae099>
- Park JD, Kim MY, Lee SG, Shin SC, Kim JH, Park IK (2009) Biological characteristics of *Lycorma delicatula* and the control effects of some insecticides. *Korean Journal of Applied Entomology* 48(1): 53–57. <https://doi.org/10.5656/KSAE.2009.48.1.053>
- Pliscoff P, Luebert F, Hilger HH, Guisan A (2014) Effects of alternative sets of climatic predictors on species distribution models and associated estimates of extinction risk: A test with plants in an arid environment. *Ecological Modelling* 288: 166–177. <https://doi.org/10.1016/j.ecolmodel.2014.06.003>
- R Core Team (2023) R: A Language and Environment for Statistical Computing. R Foundation for Statistical Computing, Vienna. <https://www.R-project.org>

- Régnière J, St-Amant R, Duval P (2012) Predicting insect distributions under climate change from physiological responses: Spruce Budworm as an example. *Biological Invasions* 14(8): 1571–1586. <https://doi.org/10.1007/s10530-010-9918-1>
- Reynolds OL, Maino J, Lye JC (2021) Spotted Lanternfly (*Lycorma delicatula*) Biology, Ecology and Awareness in the Australian Environment. Australian Plant Biosecurity Science Foundation and the Office of the Chief Environmental Biosecurity Office, Department of Agriculture, Water and the Environment, Australia, 14 pp.
- Ruzzier E, Lupi D, Tirozzi P, Dondina O, Orioli V, Jucker C, Bani L (2024) A two-step species distribution modeling to disentangle the effect of habitat and bioclimatic covariates on *Psacothaea hiliaris*, a potentially invasive species. *Biological Invasions* 26(6): 1861–1881. <https://doi.org/10.1007/s10530-024-03283-9>
- Ruzzier E, Lee S, Tirozzi P, Orioli V, Di Giulio A, Dondina O, Bani L (2025) The role of host plants, land cover and bioclimate in predicting the invasiveness of *Aromia bungii* on a global scale. *Scientific Reports* 15(1): e2353. <https://doi.org/10.1038/s41598-025-86616-5>
- Sherpa S, Renaud J, Guéguen M, Besnard G, Mouyon L, Rey D, Després L (2020) Landscape does matter: Disentangling founder effects from natural and human-aided post-introduction dispersal during an ongoing biological invasion. *The Journal of Animal Ecology* 89(9): 2027–2042. <https://doi.org/10.1111/1365-2656.13284>
- Steen B, Broennimann O, Maiorano L, Guisan A (2024) How sensitive are species distribution models to different background point selection strategies? A test with species at various equilibrium levels. *Ecological Modelling* 493: e110754. <https://doi.org/10.1016/j.ecolmodel.2024.110754>
- Thuiller W, Georges D, Gueguen M, Engler R, Breiner F, Lafourcade B, Patin R, Blancheteau H (2024) biomod2: Ensemble Platform for Species Distribution Modeling. R package version 4.2-5-2. <https://biomodhub.github.io/biomod2/>
- Urban JM (2020) Perspective: Shedding light on Spotted Lanternfly impacts in the USA. *Pest Management Science* 76(1): 10–17. <https://doi.org/10.1002/ps.5619>
- Urban JM, Leach H (2023) Biology and management of the Spotted Lanternfly, *Lycorma delicatula* (Hemiptera: Fulgoridae), in the United States. *Annual Review of Entomology* 68(1): 151–167. <https://doi.org/10.1146/annurev-ento-120220-111140>
- van Etten J (2017) R Package gdistance: Distances and Routes on Geographical Grids. *Journal of Statistical Software* 76: 1–21. <https://doi.org/10.18637/jss.v076.i13>
- Wakie TT, Neven LG, Yee WL, Lu Z (2020) The establishment risk of *Lycorma delicatula* (Hemiptera: Fulgoridae) in the United States and globally. *Journal of Economic Entomology* 113(1): 306–314. <https://doi.org/10.1093/jee/toz259>
- Wolfen MS, Binyameen M, Wang Y, Urban JM, Roberts DC, Baker TC (2019) Flight dispersal capabilities of female spotted lanternflies (*Lycorma delicatula*) related to size and mating status. *Journal of Insect Behavior* 32(3): 188–200. <https://doi.org/10.1007/s10905-019-09719-8>
- Wolfen MS, Myrick AJ, Baker TC (2020) Flight duration capabilities of dispersing adult spotted lanternflies, *Lycorma delicatula*. *Journal of Insect Behavior* 33 (2): 125–137. <https://doi.org/10.1007/s10905-020-09754-w>
- Zeller KA, McGarigal K, Whiteley AR (2012) Estimating landscape resistance to movement: A review. *Landscape Ecology* 27(6): 777–797. <https://doi.org/10.1007/s10980-012-9737-0>
- Zhang Y, Bao K, Xin B, Cao L, Wei K, Dang Y, Yang Z, Lv Z, Wang X (2023) The biology and management of the invasive pest Spotted Lanternfly, *Lycorma delicatula* (White) (Hemiptera: Fulgoridae). *Journal of Plant Diseases and Protection* 130(6): 1155–1174. <https://doi.org/10.1007/s41348-023-00794-w>
- Zhao Z, Yang L, Chen X (2024) Globally suitable areas for *Lycorma delicatula* based on an optimized Maxent model. *Ecology and Evolution* 14(9): e70252. <https://doi.org/10.1002/ece3.70252>

Supplementary material 1

Supplementary tables

Authors: Enrico Ruzzier, Davide Scaccini, Pietro Tirozzi, Valerio Orioli, Olivia Dondina, Andrea Di Giulio, Alberto Pozzebon, Luciano Bani

Data type: xlsx

Explanation note: **table S1**. Schematic associations between the host plant taxon and land cover.

table S2. Evaluation HSM. Table of the three evaluation metrics used for HSM. **table S3**. Evaluation BSM. Table of the three evaluation metrics used for BSM. **table S4**. Importance of the covariates included in the HSM. **table S5**. Importance of the covariates included in the BSM.

Copyright notice: This dataset is made available under the Open Database License (<http://opendata-commons.org/licenses/odbl/1.0/>). The Open Database License (ODbL) is a license agreement intended to allow users to freely share, modify, and use this Dataset while maintaining this same freedom for others, provided that the original source and author(s) are credited.

Link: <https://doi.org/10.3897/neobiota.103.154246.suppl1>

Supplementary material 2

Supplementary figures

Authors: Enrico Ruzzier, Davide Scaccini, Pietro Tirozzi, Valerio Orioli, Olivia Dondina, Andrea Di Giulio, Alberto Pozzebon, Luciano Bani

Data type: pdf

Explanation note: **fig. S1**. Distribution of the 20 sets of PAs + BPs used for the habitat suitability model (HSM) calibration in the narrow native calibration range. **fig. S2**. Distribution of the 5 sets of BPs used for the bioclimatic suitability model (BSM) calibration in the wide calibration range. **fig. S3**. Response curves of covariates included in the *Lycorma delicatula* habitat suitability models (HSM). **fig. S4**. Response curves of covariates included in the *Lycorma delicatula* bioclimatic suitability models (BSM). **fig. S5**. Habitat suitability map for *Lycorma delicatula* in the narrow native calibration range obtained projecting the habitat suitability model (HSM). **fig. S6**. Bioclimatic suitability map for *Lycorma delicatula* in the wide calibration range obtained projecting the bioclimatic suitability model (BSM). **fig. S7**. Overall suitability map for *Lycorma delicatula* in the narrow native calibration range. **fig. S8**. Boyce of the overall suitability map for *Lycorma delicatula* in the narrow native calibration range. **fig. S9**. Global (a) HSM and (b) BSM Multivariate Environmental Similarity Surfaces (MESS) index. **fig. S10**. Overall suitability map for *Lycorma delicatula* in the Eastern USA. In red species occurrences. **fig. S11**. Boyce of the overall suitability map for *Lycorma delicatula* in the Eastern USA. **fig. S12**. Overall suitability map for *Lycorma delicatula* in South Korea. In red species occurrences. **fig. S13**. Boyce of the overall suitability map for *Lycorma delicatula* in South Korea. **fig. S14**. World projections of *Lycorma delicatula* suitability maps; a) habitat suitability map; b) bioclimatic suitability map. **fig. S15**. Eastern and southeast Asia (ESA) projections of *Lycorma delicatula* suitability maps. **fig. S16**. USA projections of *Lycorma delicatula* suitability maps. **fig. S17**. Details of USA (East Coast) projections of *Lycorma delicatula* suitability maps. **fig. S18**. European projections of *Lycorma delicatula* suitability maps.

Copyright notice: This dataset is made available under the Open Database License (<http://opendata-commons.org/licenses/odbl/1.0/>). The Open Database License (ODbL) is a license agreement intended to allow users to freely share, modify, and use this Dataset while maintaining this same freedom for others, provided that the original source and author(s) are credited.

Link: <https://doi.org/10.3897/neobiota.103.154246.suppl2>